Published in final edited form as:
J Proteome Res. 2008 August ; 7(8): 3447–3460. doi:10.1021/pr800187n.

Global Impact of Oncogenic Src on a Phosphotyrosine Proteome

Weifeng Luo[†], **Robbert J. Slebos**[‡], **Salisha Hill**[⊥], **Ming Li**[§], **Jan Brábek**[○], **Ramars Amanchy**[∇,#], **Raghothama Chaerkady**[∇,♦], **Akhilesh Pandey**[∇], **Amy-Joan L. Ham**[‖,⊥], and **Steven K. Hanks**

†*Department of Cell and Developmental Biology, Vanderbilt University School of Medicine, Nashville, Tennessee 37232*

‡*Department of Cancer Biology, Vanderbilt University School of Medicine, Nashville, Tennessee 37232*

⊥*The Proteomics Laboratory of the Mass Spectrometry Research Center, Vanderbilt University School of Medicine, Nashville, Tennessee 37232*

§*Department of Biostatistics, Vanderbilt University School of Medicine, Nashville, Tennessee 37232*

○*Department of Cell Biology, Charles University, Prague, Czech Republic*

∇*McKusick-Nathans Institute of Genetic Medicine and the Departments of Biological Chemistry, Oncology and Pathology, Johns Hopkins University, Baltimore, Maryland 21205*

♦*Institute of Bioinformatics, International Technolgy Park, Bangalore, 560066, India*

‖*Department of Biochemistry, Vanderbilt University School of Medicine, Nashville, Tennessee 37232*

Abstract

Elevated activity of Src, the first characterized protein-tyrosine kinase, is associated with progression of many human cancers, and Src has attracted interest as a therapeutic target. Src is known to act in various receptor signaling systems to impact cell behavior, yet it remains likely that the spectrum of Src protein substrates relevant to cancer is incompletely understood. To better understand the cellular impact of deregulated Src kinase activity, we extensively applied a mass spectrometry shotgun phosphotyrosine (pTyr) proteomics strategy to obtain global pTyr profiles of Src-transformed mouse fibroblasts as well as their nontransformed counterparts. A total of 867 peptides representing 563 distinct pTyr sites on 374 different proteins were identified from the Src-transformed cells, while 514 peptides representing 275 pTyr sites on 167 proteins were identified from nontransformed cells. Distinct characteristics of the two profiles were revealed by spectral counting, indicative of pTyr site relative abundance, and by complementary quantitative analysis using stable isotope labeling with amino acids in cell culture (SILAC). While both pTyr profiles are replete with sites on signaling and adhesion/cytoskeletal regulatory proteins, the Src-transformed profile is more diverse with enrichment in sites on metabolic enzymes and RNA and protein synthesis and processing machinery. Forty-three pTyr sites (32 proteins) are predicted as major biologically relevant Src targets on the basis of frequent identification in both cell populations. This select group, of particular interest as diagnostic biomarkers, includes well-established Src sites on signaling/adhesion/cytoskeletal proteins, but also uncharacterized sites of potential relevance to the transformed cell phenotype.

Keywords

cell transformation; mass spectrometry; signal transduction; tyrosine kinase

*To whom correspondence should be addressed. Tel, 615-343-8502; fax, 615-936-5673; e-mail, steve.hanks@vanderbilt.edu.
#Present address: Department of Genome Science, Genome Research Institute, University of Cincinnati, Cincinnati, OH 45237, USA.

Introduction

The discovery that the oncogene v-*src* encodes a tyrosine-specific protein kinase[1] led eventually to the recognition of tyrosine phosphorylation as a major metazoan cell regulatory mechanism. Oncogenic variants of Src have constitutive kinase activity that causes "transformation", the acquisition of neoplastic properties including proliferative independence from anchorage and growth factors, altered morphology, and high invasive capacity.[2,3] Although activating Src mutations are rarely associated with human cancer, elevated Src activity is nonetheless commonly observed in tumors and there is current interest in Src as a therapeutic target.[4,5]

Since the discovery of Src's tyrosine kinase activity over 25 years ago, there has been sustained effort to identify its protein substrates in order to understand both normal signaling functions and how deregulated activity gives rise to transformation. The emergent picture is of a potent enzyme that interacts with multiple receptor systems (e.g., cell-extracellular matrix (ECM) adhesions, cell-cell adherens junctions, receptor tyrosine kinases, and G protein-coupled receptors) to participate in signaling responses to a variety of extracellular cues.[3,6–9] Under conditions of elevated Src activity, enhanced and/or aberrant phosphorylation of its substrates at such signaling centers is thought to contribute to transformation and malignant cancer progression.

While dozens of Src substrates have been identified,[3,10,11] an understanding of how Src transforms cells is still incomplete. Recently, Rush et al.[12] developed a shotgun proteomics approach, involving immunoaffinity enrichment for peptides containing phosphotyrosine (pTyr) with analysis by liquid chromatography-tandem mass spectrometry (LC-MS/MS). This approach has potential to greatly extend knowledge of the cellular impact of oncogenic Src, and an initial application of the strategy to Src-transformed fibroblasts identified 185 distinct pTyr sites representing 128 different proteins, including many previously unrecognized targets of tyrosine phosphorylation.[12]

In this report, we have extensively applied the pTyr shotgun proteomics strategy to both Src-transformed mouse embryo fibroblasts (MEFs) and counterpart nontransformed MEFs in order to obtain a more complete understanding of how deregulated Src activity impacts the global pTyr state of these cells. A spectral counting approach indicating pTyr site relative abundance was complemented by SILAC (stable isotope labeling with amino acids in cell culture) to reveal distinct characteristics of the Src-transformed pTyr profile, including enrichment in sites on metabolic enzymes and machinery for RNA and protein synthesis and processing. Forty-three pTyr sites readily detected in both cell populations, including many not previously characterized, are presented as potentially useful biomarkers of elevated Src activity impacting on the transformed phenotype.

Experimental Methods

Cells and Cell Culture

The Src-transformed and counterpart nontransformed cell populations used in this study have been described previously.[13] Both populations were derived from p130Cas −/− MEFs, whereby either oncogenic Src-F529 (for Src-transformed cells) or the empty retroviral vector (for nontransformed cells) was first introduced, followed by separate retroviral-mediated reconstitution of p130Cas expression in each of the resulting cell populations. P130Cas expression in the nontansformed cells is equivalent to the level of the endogenous protein, which is ~3-fold higher than was achieved in the Src-transformed cells.[13] Both cell populations

were maintained under standard culture conditions in 10% FBS, and their pTyr proteomes were assessed from cells actively growing and motile at ~75% confluency.

Sample Preparation and Analysis by LC-MS/MS

For each round of analysis, pTyr peptides were enriched from 2.5 $\times 10^8$ cells according to the protocol of Rush et al.,[12] with either anti-pTyr antibody PY100 (Cell Signaling Technology, Danvers, MA) or 4G10 (Millipore, Billerica, MA) used as immunoaffinity agent. Preparations involving PY100 employed the PhosphoScan kit (Cell Signaling Technology). Chymotryptic peptides were obtained by treating lysates for 4 h at 25 °C with chymotrypsin-TLCK (Worthington, Lakewood, NJ) at a 60:1 cellular protein/chymotrypsin ratio.

LC-MS-MS analysis of immunoaffinity-purified peptides was performed using a Thermo LTQ ion trap mass spectrometer equipped with a Thermo MicroAS autosampler and Thermo Surveyor HPLC pump, Nanospray source, and Xcalibur 1.4 instrument control. The peptides were separated on a packed capillary tip, 100 mm × 11 cm, with C18 resin (Jupiter C_{18}, 5 μm, 300 Å, Phenomonex, Torrance, CA) using an inline solid phase extraction column that was 100 mm × 4 cm packed with the same C18 resin (using a frit generated with liquid silicate Kasil 1[14] similar to that previously described,[15] except the flow from the HPLC pump was split prior to the injection valve. The flow rate during the solid phase extraction phase of the gradient was 1 μL/min and during separation phase was 700 nL/min. Mobile phase A was 0.1% formic acid, mobile phase B was acetonitrile with 0.1% formic acid. A 95 min gradient was performed with a 15 min washing period diverted to waste after the precolumn (100% A for the first 10 min followed by a gradient to 98% A at 15 min) to allow for solid phase extraction and removal of any residual salts. After the initial washing period, a 60 min gradient was performed where the first 35 min was a slow, linear gradient from 98% A to 75% A, followed by a faster gradient to 10% A at 65 min and an isocratic phase at 10% A to 75 min. MS/MS scans were acquired using an isolation width of 2 *m*/*z*, and activation time of 30 ms, activation Q of 0.250, and 30% normalized collision energy using 1 microscan and maximum injection time of 100 for each scan. The mass spectrometer was tuned prior to analysis using the synthetic peptide TpepK (AVAGKAGAR). Typical tune parameters were as follows: spray voltage of 1.8 kV, a capillary temperature of 160 °C, a capillary voltage of 50 V and tube lens of 100 V. The MS/MS spectra of the peptides were acquired using data-dependent scanning in which one full MS spectra, using a full mass range of 400–2000 amu, was followed by 5 MS/MS spectra. Incorporated into the method was a data-dependent scan for the neutral loss of phosphoric acid or phosphate (−98, −80), such that if these masses were found, an MS/MS/MS of the neutral loss ion was performed.

Database Searching, Filtering, and False-Discovery Rate Determination

The “ScanDenser” algorithm read tandem mass spectra stored as centroided peak lists from Thermo RAW files and transcoded them to DTA files. Spectra that contained fewer than 25 peaks or that had less than 2e1 measured total ion current did not result in DTAs. Singly charged DTAs were created if the 90% of the total ion current occurred below the precursor ion, and all other spectra were processed as both doubly and triply charged DTAs Proteins were identified using the TurboSEQUEST v.27 (rev. 12) algorithm[16] (Thermo Electron, San Jose, CA) and the mouse subset of the December 2005 release of the UniRef100 database (www.uniprot.org) containing 87 226 sequences. The database was reversed so that false-discovery rates could be determined and the reversed version of each protein sequence was appended to the forward database for a total of 174 452 sequences. The searches were performed allowing the following differential modifications: +57 on cysteine (for carboxyimidomethylation from iodoacetamide), +16 on methionine (oxidation), and +80 on Ser, Thr, or Tyr (phosphorylation). The MS/MS/MS spectra were also searched for a −18 mass shift on Ser, Thr, or Tyr to account for the loss of water which results from the neutral loss of

phosphoric acid. Peptide and fragment ion tolerances were set to 2.5 and 1.0 Da, respectively. Protein matches were preliminarily filtered using the following criteria: if the charge state of the peptide is 1, the xcorr is greater than or equal to 1, the RSp is less than or equal to 5, and the Sp is greater than or equal to 350. If the charge state is 2, the xcorr is greater than or equal to 1.8, the RSp is less than or equal to 5, and the Sp is greater than or equal to 350. If the charge state is 3, the xcorr is greater than or equal to 2.5, the RSp is less than or equal to 5, and the Sp is greater than or equal to 350. Once filtered based on these scores, all peptides were required to contain a tyrosine and a phosphorylation. A final filter then retained only pTyr-containing peptides meeting at least one of three additional criteria: (1) at least two matching spectra had xcorr values above a high threshold (≥3.3 for charge of 3, ≥2.2 for charge of 2, and ≥1.5 for charge of 1), (2) the pTyr site was independently identified from two or more distinct peptides, or (3) the pTyr site had been independently identified elsewhere and included in the PhosphoSite online resource of *in vivo* phosphorylation sites, version 1.5 (http://www.phosphosite.org), maintained by Cell Signaling Technology, Inc. False-discovery rates were estimated from peptide matches to the reverse database in which the total number of reverse peptides were multiplied by two and divided by the total number of peptide hits after the application of the filtering criteria.

Determination of "Highly Enriched" Sites

A modified peptide frequency-based analysis approach based on comparing peptide spectral identifications between groups[17] was used to determine pTyr sites that were identified with significantly higher frequency in one cell population relative to the other. The unit of measure was the number of times a peptide carrying a specific pTyr site was observed in a single LC-MS/MS round of analysis. These totals were tabulated for all peptides observed for each of the 36 LC-MS/MS rounds (18 for each cell population). For the purpose of this group comparison, the experimental differences between the LC-MS/MS rounds due to the use of two different cleaving agents or two phosphotyrosine antibodies can be ignored since they are identical between the two cell populations. A Poisson regression model was applied to detect spectral count differences between the two groups for each pTyr site. The False Discovery Rates (FDR) approach was used to handle large-scale simultaneous hypothesis testing. Sites with FDR adjusted $p < 0.01$ were considered significantly different in detection frequency, or "highly enriched" in one cell population relative to the other.

SILAC Analysis

The SILAC labeling strategy[18] was used for relative quantitation of phosphotyrosine peptides. Nontransformed cells were grown in regular DMEM and Src-transformed cells were adapted to SILAC-specific DMEM containing $^{13}C_6$-arginine and $^{13}C_6$-lysine in 10% FBS. Stable heavy isotope containing amino acids $^{13}C_6$-arginine and $^{13}C_6$-lysine were obtained from Cambridge Isotope Labs (Andover, MA). A detailed protocol for SILAC media preparation is available at http://www.silac.org. Phosphotyrosine-containing peptides were purified from cells growing at ~80% confluence using the PhosphoScan Kit (Cell Signaling Technology, Danvers, MA) as per the manufacturer's instruction. The peptides were dried and reconstituted in 10 μL of 0.2% formic acid and analyzed using reversed phase nanoscale liquid chromatography on a QSTAR Pulsar (Applied Biosystems-MDS Sciex) quadrupoletime-of-flight mass spectrometer. The mass spectrometer was interfaced with an Eksigent (Monmouth Junction, NJ) nanoLC system consisting of a trap column (75 μm × 3 cm, C18 material 5–10 μm, 120Å; YMC, Kyoto, Japan) and an analytical column (75 μm × 10 cm, C18 material 5 μm, 120Å; YMC) with an emitter tip of 8 μM (New Objective, Woburn, MA) attached. The peptides were eluted using an organic solvent gradient from 5 to 40% acetonitrile in 0.1% formic acid, for 30 min with a flow rate of 300 nL/min. The MS spectra (*m*/*z* 350–1200 range) were acquired in a data-dependent manner targeting the three most abundant ions in the survey scan using a dynamic exclusion of 45 s. The identification and quantitation of phosphopeptide was done

after formatting the mass spectrometry data. LC-MS/MS data acquired using AnalystQS 1.1 (MDS Sciex, Concord, Canada) were searched using Mascot v2.2.0 (Matrixscience, Manchester, U.K.) against RefSeq 26 database (date created Nov 04, 2007), mouse subset containing 20 311 sequences. The reverse database RefSeq26r was also searched and the false-discovery rate was 0%. While searching the database, carbamidomethylation of cysteine was set as a fixed modification and phosphorylation of tyrosine, serine, and threonine, arginine $^{13}C_6$, lysine $^{13}C_6$, oxidation of methionine were permitted as variable modifications. The mass tolerance was set at 0.2 amu for precursor and 0.5 amu for fragmented ions. Relative quantitation of phosphotyrosine peptides was performed using MSQuant downloaded from http://msquant.sourceforge.net,[19] which computes protein quantitation ratios along with standard deviation. Essentially, Mascot search results were parsed with LC-MS/MS instrument data file using MSQuant. The quantitation data was verified by manual inspection of heavy and light peptide derived MS and MS/MS spectra in all cases.

Immunoblotting

Immunoblot analyses of total cell lysates were carried out by standard methods, using primary rabbit antibodies, HRP-conjugated goat anti-rabbit secondary, and detection by ECL. The phospho-ERK1/2 (p44/42 MAP kinase T202/Y204), phospho-FAK (Tyr576/577), and phospho-p85 (Tyr467), antibodies were obtained from Cell Signaling Technology. Antibodies against total ERK1 (K-23), total ERK2 (C-14) and total FAK (C-20) were from Santa Cruz Biotechnology. Total ERK1/2 was detected using an equal mixture of the K-23 and C-14 antibodies. Antibodies against total RIN-1 and RIN-1 pTyr-35 were provided by John Colicelli (UCLA).

Results and Discussion

Phosphotyrosine Profiles from Nontransformed versus Src-Transformed Cells Obtained through Extensive Application of a Shotgun Proteomics Strategy

We analyzed the global pTyr state of a population of MEFs that express oncogenic mouse Src-F529 in which the negative regulatory Tyr-529 was changed to phenylalanine. These cells have greatly elevated cellular pTyr levels and properties classically associated with Src-transformation including anchorage-independent growth, altered morphology, formation of podosome rosettes, and invasive/metastatic behavior.[13,20] To assess the impact of Src-F529, a parallel analysis was performed on a counterpart population of nontransformed cells. The shotgun pTyr proteomics strategy[12] was applied in large scale through 18 rounds of analysis for each cell type, including 10 biological replicates with peptides generated by trypsin and 8 biological replicates with cleavage by chymotrypsin. Peptides were enriched using either or two different anti-pTyr antibodies, PY100 or 4G10, with each antibody used for half of the replicates. Resulting peptides were analyzed by LC-MS/MS with spectra matching against the mouse subset of the UniRef100 database. Figure 1 shows representative annotated spectra for four pTyr-containing peptides, representing four different proteins (additional representative annotated spectra are presented in Supplemental Figure S1). After applying filtering criteria, a total of 867 unique peptides representing 563 distinct pTyr sites on 374 different proteins were retained from the analysis of Src-transformed cells, while 514 unique peptides representing 275 pTyr sites on 167 proteins were retained from the nontransformed cells (Figure 2A). Searching the spectra against the sequence-reversed database, while employing the same criteria for data retention, gave an estimate of false-discovery rates as less than 1.5%.

All retained peptides for the nontransformed and Src-transformed cells are listed in Supplemental Table S1 and Supplemental Table S2, respectively, and organized according to a functional classification of the represented proteins. These tables also include information on the amino acid position of the pTyr site, tallies of independent spectral counts, highest cross-

correlation (xcorr) values for each peptide and charge state with associated precursor ion mass and second-ranking peptides with delta correlation (dCn) values >0.2. Inspection of these tables indicates that the chymotryptic digests revealed several sites not detected in tryptic digests and provided critical confirmation for others. The two anti-pTyr antibodies generated similar data, with little distinction in their abilities to recover pTyr peptides.

Multiple distinct peptides were identified for 111 (40%) of the nontransformed cell pTyr sites and for 203 (36%) of the sites identified from the Src-transformed cells. Of the sites represented by single phosphopeptides, the large majority were retained on the basis of multiple independent identifications with at least two xcorr values meeting the retention threshold of ≥3.3 for charge of 3, ≥2.2 for charge of 2, and ≥1.5 for charge of 1. In addition, we chose to include in the final data set 32 pTyr sites from nontransformed cells and 90 sites from Src-transformed cells that were identified only once from our 36 combined rounds of analysis but which have been reported in the PhosphoSite online resource of *in vivo* phosphorylation sites. This latter group includes some well-established pTyr sites, but is also more likely to include misidentified sites. Plots of identification frequencies (combined spectral counts) for all pTyr sites retained approximate the Poisson distribution (Figure 2B). The numbers of distinct sites (and proteins) are reduced by about half when only sites with four or more independent identifications are considered (Figure 2A).

An advantage of using an ion trap mass spectrometer for these studies is that the adjustable injection time can increase the sensitivity and improve the quality of the MS/MS spectrum, thus, enhancing the capacity of spectral counting to evaluate differences in the two cell populations. In comparing the nontransformed versus Src-transformed pTyr profiles, however, it became clear that a limitation of the shotgun approach in this particular application was the data-dependent acquisition step during MS/MS, which tends to select only the most intense peptide ions for analysis. While ions once detected are excluded from fragmentation to enhance the identification of lower level ions, large differences in sample complexity can still impact on the comparison. The pTyr peptide preparations from the Src-transformed cells are necessarily much more complex than the preparations from nontransformed cells (producing many more intense signals), such that peptides representing sites phosphorylated to similar extents in both populations will be relatively less abundant in the Src-transformed preparation and therefore less likely selected for MS/MS analysis. For this reason, observed differences between the two cell populations in a site's identification frequency cannot be used as an absolute quantitative measure of the relative differences in phosphorylation stoichiometry. Nevertheless, the site identification frequency can be taken as an indicator of peptide relative abundance in each of the pTyr-enriched preparations and thus a useful statistic for assessing the global impact of oncogenic Src. Later in this report, we present an independent quantitative analysis using the SILAC approach.

The pTyr Profiles Obtained from Nontransformed versus Src-Transformed Cells Have Distinct Characteristics

Of the 563 sites detected from Src-transformed cells, only 123 were also detected in the nontransformed cells (Figure 2C, left). The nontransformed cells also have a specific profile, with 152 sites detected exclusively in this population. Thus, from the two populations combined, 715 total pTyr sites (representing 458 different proteins) were identified. Many of the sites (the majority from Src-transformed cells) have not previously been described in the published literature and/or remain functionally uncharacterized. The largely distinct natures of the two profiles are maintained when the data are limited to more frequently identified sites, exemplified by those found ≥4 times (Figure 2C, right).

The rather distinct characteristics of the two profiles are further evident from the functional classification of represented proteins (Figure 3A, and see Supplemental Table S1 and

Supplemental Table S2). From nontransformed cells, about half of the sites are on proteins classified under the broad "Signaling" category and another 25% on proteins in the "Adhesion/Cytoskeleton" category. Considering only those sites with ≥4 identifications resulted in further enrichment in these categories (Figure 3B, left). By comparison, the Src-transformed profile was more broadly distributed, with the Signaling and Adhesion/Cytoskeleton categories together comprising less than half of the total and with large representations of proteins classified under RNA Synthesis and Processing, Protein Synthesis and Processing, and Others of miscellaneous or unknown function (Figure 3A, right). For Src-transformed cells, limiting the analysis to sites identified ≥4 times has little effect on these distributions (Figure 3B). The distinct characteristics of the two profiles are also readily apparent from inspection of the most frequently identified sites (Table 1). Most frequently detected in the nontransformed cells is pTyr-15 on CDK1, a target of a dual-specificity kinase that maintains this cyclin-dependent kinase in an inactive state during interphase.[21] From Src-transformed cells, most frequently detected is pTyr-24 on the glycolytic enzyme enolase, one of the first documented v-Src substrates.[22]

To further evaluate differences between the two profiles, a statistical permutation test based on the Poisson distribution was used to display sites detected with significantly higher frequency ($p < 0.01$) in one cell type versus the other. With this test, 70 sites on 56 proteins were judged as being comparatively "highly enriched" in the nontransformed cell preparations, while 51 sites on 42 proteins were highly enriched in Src-transformed cell preparations (Table 2 and Table 3, respectively). For nontransformed cells, such sites fall almost entirely in the Signaling and Adhesion/Cytoskeleton categories, but for the Src-transformed cells, these categories were reduced through considering only the highly enriched sites (Figure 3C). The frequently identified (Table 1) and highly enriched (Table 2 and Table 3) sites provide some focus for the following discussions of prominent features of the two pTyr profiles.

Prominent Features of the pTyr Profile Obtained from Nontransformed Cells

Sites on protein kinases account for 30 of the 70 highly enriched sites in the nontransformed cell profile. Included are sites on 12 traditional tyrosine kinases and 10 other proten kinases in the phylogenetic "CMGC" group.[23] Highly enriched sites on CMGC kinases CDK1, GSK3, ERK1, ERK2, p38α, DYRK1A, and PRP4 are also among those most frequently identified from these cells. GSK3β pTyr-216 (not distinguishable from GSK3α), an important site of activation loop autophosphorylation during protein folding,[24] is the second most frequently identified in nontransformed cells. The activation loop sites identified on the related dual-specificity kinases DYRK1A and PRP4 are likely also sites of autophosphorylation during maturation, as demonstrated for Drosophila DYRK family members.[25] The sites on ERK1, ERK2 and p38α are also activation loop sites, targeted by other dual-specificity kinases, that reflect the active states of these MAPKs. Other CMGC kinases represented by nontransformed cell highly enriched sites are ERK5 and dual-specificity kinases HIPK1 and HIPK3.

Among traditional tyrosine kinases, focal adhesion kinase (FAK) stands out in the nontransformed cell profile with 3 highly enriched sites: pTyr-397, pTyr-576, and pTyr-577. FAK Tyr-397 is a site of autophosphorylation in response to cell-ECM adhesion, and Src is recruited to this site to phosphorylate FAK activation loop tyrosines 576 and 577.[26] Activation of the FAK/Src complex influences adhesion/cytoskeletal dynamics and is important for efficient cell motility.[6,26] Further reflecting the prominence of cell-ECM adhesion signaling in the nontransformed cell profile are highly enriched sites on two major substrates of the FAK/Src complex, paxillin (pTyr-88 and pTyr-118) and p130Cas (pTyr-238 and pTyr-253), that serve to dock downstream signaling effectors.[26] FAK pTyr-576, paxillin pTyr-118, and p130Cas pTyr-253 are among the most frequently identified in these cells. P130Cas expression is known to enhance Src-mediated phosphorylation of certain adhesion/cytoskeletal proteins

including FAK and paxillin.[20] The ~3-fold higher level of p130Cas expression in the nontransformed versus the Src-transformed cells[13] could therefore have accounted for some of the enrichment of cell/ECM adhesion proteins in the nontransformed cell profile. Other nontransformed cell highly enriched sites are on proteins implicated in regulating the adhesion-actin cytoskeletal network, including p190RhoGAP pTyr-943[27] and protein-tyrosine phosphatase PTPα pTyr-825.[28] Highly enriched sites on other cell-ECM adhesion proteins (tensin, vinculin), cell–cell adhesion proteins (p120catenin, plakophilin-4, PARD3), and others (CrkL, RhoGAP-12, BCAR3, N-WASP) may also impact adhesion–cytoskeletal dynamics. In addition to FAK, nonreceptor tyrosine kinases are further represented by highly enriched regulatory sites on members of the Src family and on ACK that is activated in response to both cell-ECM adhesion and growth factors.[29]

Receptor tyrosine kinases figure prominently in the nontransformed cell profile. Sites were detected on 7 members of the Eph receptor family including highly enriched sites on EphA2 and EphB3. Bidirectional signaling from Eph receptors and their transmembrane ephrin ligands regulate cytoskeletal, adhesive, and motile properties of interacting cells.[30] One Eph receptor ligand, ephrin B2 (most peptides common to ephrin B1), was also part of the nontransformed cell profile with multiple sites identified including one highly enriched site. Also highly enriched are activation loop sites on receptor tyrosine kinases Met, Axl, DDR2, and IGF1R. The docking protein Dok1, a downstream target of various receptor and nonreceptor tyrosine kinases, is prominent in the nontransformed cell profile with five sites identified. Dok1 pTyr-361, the only site ranking among the 10 most frequently identified in both populations, is important for recruitment of the adaptor Nck to stimulate F-actin reorganization and cell motility.[31,32] Other downstream effectors for receptor tyrosine kinases that are represented by nontransformed cell highly enriched sites are adaptor/docking proteins LAP2, Shb, Shc1, Gab1, and insulin receptor substrate 2. Other notable signaling/regulatory proteins represented by nontransformed cell highly enriched sites are caveolin-2, calmodulin, and STAT3.

In summary, the pTyr profile of the nontransformed cell population strongly reflects the receptor- and adhesion-associated signaling pathways the act to drive proliferative and motile cell behavior.

Prominent Features of the Src-Transformed Cell pTyr Profile

A major distinction of the Src-transformed profile is an absence of protein kinases, other than Src itself, in the lists of sites either most frequently identified or highly enriched. Two sites on Src, pTyr-92 and pTyr-438, are highly enriched in the transformed cells, and remarkably, both are essentially uncharacterized. Tyr-92 is a conserved residue in the SH3 domain that has an important role in ligand binding.[33] Tyr-438 is in a region of the kinase domain implicated in substrate selection, and has been previously described as an autophosphorylation site in studies on a recombinant kinase domain.[34] A third novel site on Src, detected at low frequency, is Tyr-231 in the SH2 domain. These findings suggest that oncogenic Src has the capacity to undergo more extensive autophosphorylation than previously appreciated, with implications for regulation of substrate selection. While no other sites on protein kinases made the lists of highly enriched or most frequently identified, these signaling enzymes are nevertheless well-represented in the Src-transformed profile with 30 additional sites representing 20 protein kinases. Included are the sites on FAK, EphA2, CDK1, GSK3, and PRP4 that were frequently detected in nontransformed cells.

It is notable that sites on several other protein kinases that were very frequently detected in the nontransformed cells are absent in the Src-transformed profile, including those on Met, ACK, ERK1, ERK2, and p38α. The limitation of shotgun proteomics imposed by data-dependent acquisition is clearly a factor in the comparatively low-frequency identification in Src-transformed cells of such pTyr sites that are not known or not likely to be directly targeted by

the oncogenic Src kinase. As an illustration of this point, the ERK1/ERK2 activation loop sites are still quite readily detected in the Src-transformed cells and nontransformed cells through immunoblotting with phosphospecific antibodies (Figure 4A), although the signal is reduced in comparison to the nontransformed cells. A more revealing example of the sensitivity limitation is the FAK activation loop. Immunoblotting shows that FAK activation loop phosphorylation is elevated in the Src-transformed cells (Figure 4B), as expected for this recognized Src target, although the acivtion loop sites were detected by the shotgun proteomics approach with significantly higher frequency in the nontransformed cells.

Other Signaling and Adhesion/Cytoskeleton proteins make notable contributions to the Src-transformed cell profile. Annexins, which are calcium-dependent phospholipid-binding proteins involved in structural organization and intracellular signaling, are well-represented by annexins A1, A2, A5, A6, and A11. Annexin A2 pTyr-274 and annexin A6 pTyr-29 are highly enriched sites. Four additional sites were detected on annexin A2, the first identified v-Src substrate previously known as p36 calpactin I/lipocortin II,[35] including pTyr-23 also found in nontransformed cells. Other sites detected multiple times in Src-transformed cells, but absent in the nontransformed profile, are on signaling proteins phospholipase Cγ1, Rab GDIβ, RACK1 (receptor of activated protein kinase C), striatin-3, and Tks4 (related to Tks5/FISH). Cell-ECM adhesion-associated proteins including p130Cas, LPP (lipoma preferred partner), paxillin, talin, tensin, vinculin, and VASP were readily detected, with several previously unrecognized sites among the many identified on these proteins. On vinculin, the first cytoskeletal substrate identified for v-Src,[36] pTyr-99 is highly enriched. Similarly, cell–cell adhesion proteins contributed to the Src-transformed profile including p120catenin, PARD3, plakophilin-4, ZO-1, and ZO-2, again with several novel sites detected. Actin regulators are notably represented by sites on cofilin, cortactin, and by a highly enriched site on actin interacting protein AIP1. Intriguing novel sites were found on three components (Arp2, Arp3, and p21Arc) of the Arp2/3 complex that acts to nucleate new actin filaments. Arp2 pTyr-91 and p21Arc pTyr-46 are among the highly enriched sites. Other readily detected sites include actin cross-linkers α-actinin and filamin B, and cytokinesis regulators anillin and septin-2. Sites on α-actinin, filamin B, and plectin (a cross-linker of microtubules to intermediate and actin filaments) are among those highly enriched.

The Src-transformed profile includes many metabolic enzymes including several involved in glycolysis. In addition to enolase with two of the three most frequently identified sites, glycolytic enzymes are represented by GAPDH, phosphofructokinase, lactate dehydrogenase, phosphoglycerate mutase, and pyruvate kinase isoform M2. Glycolytic enzyme pTyr sites are of interest in light of findings implicating tyrosine phosphorylation in the switch from oxidative phosphorylation to aerobic glycolysis (the “Warburg effect”) that is important for cancer cell metabolism and tumor growth. Of particular note in this context are recent studies showing that the Warburg effect can result as a consequence of pyruvate kinase M2 binding to pTyr-binding peptides, including sites identified on enolase (pY43) and lactate dehydrogenase (pY238), which inhibits pyruvate kinase M2 enzymatic activity to divert glucose metabolites to anabolic processes.[37,38] GAPDH and the rate-limiting phosphofructokinase have previously been characterized as substrates for the EGF receptor[39] prompting speculation that these phosphorylation events could contribute to the altered energy metabolism in cancer cells. Sites on over a dozen other diverse metabolic/biosynthetic enzymes were detected in the Src-transformed cells, including several additional highly enriched sites.

Proteins involved in RNA and protein synthesis and processing are a major aspect of the Src-transformed cell profile. Included are many RNA helicases, hnRNPs, splicing factors, tRNA synthetases, ribosomal proteins, translation initiation factors, chaperones, and components of the ubiquitin–proteasome system. Proteins in these categories also account for a large fraction of the Src-transformed cell frequently identified and highly enriched sites. The second most

frequently detected site in the Src-transformed cells is pTyr-485 on hnRNP Q, almost all from chymotryptic peptides. The DEAD-box RNA helicase, DDX3X, emerges as a prominent likely target of oncogenic Src, with 7 distinct sites detected including one of the most frequently identified. Tyrosine phosphorylation of proteins that function in RNA processing may account for past observations of oncogenic Src activity causing partially spliced transcripts to accumulate in the nucleus.[40] Also among the most frequently identified in Src-transformed cells are two sites on proteasome subunit PSMA2.

To summarize, a distinguishing aspect of the Src-transformed cell profile is the large representation of proteins having basic "housekeeping" functions including metabolic enzymes and macromolecular synthetic machinery. For pTyr sites on such abundant cellular proteins that were detected only in the Src-transformed cells, it must be considered that these may not be normal targets of endogenous tyrosine kinases but rather represent superfluous targets of the catalytically potent oncogenic Src "*gone wild*". Nevertheless, such sites could have an impact on the neoplastic properties of these cells.

P-Tyr Sites Identified Frequently in Both Nontransformed and Src-Transformed Cells

Considering once again the limitations of data-dependent acquisition in profiling the Src-transformed cells, pTyr sites that were frequently identified in both cell populations are likely to include the major (most abundant) biologically relevant Src sites. That is, such sites are likely to be prominently phosphorylated in normal cells but also undergo elevated phosphorylation in the presence of oncogenic Src. Forty-seven sites, representing 36 proteins, met the arbitrary cutoff of ≥4 identifications in each cell type. Four of these sites, on CMGC kinases CDK1, GSK3β, DYRK1A, and PRP4, are among those most frequently identified in the nontransformed cells (Table 2) while being identified with greatly reduced frequencies in Src-transformed cells, which is consistent with these sites not being direct Src targets.

The remaining 43 sites representing 32 proteins (Table 4) we consider as candidate Src substrates (see Supplemental Figure S1 for representative annotated spectra of peptides containing these sites, and Supplemental Text File for brief overviews of these proteins focused on their tyrosine phosphorylation). For 23 of these proteins (red highlighting in Table 4), the existing evidence supports them as being *bona fide* Src substrates. Src is on this list by virtue of its activation loop autophosphorylation site, and also represented are other established Src sites on FAK, p130Cas, paxillin, p120catenin, SHIP2, p190RhoGAP, caveolin-1, cortactin, Nck1, Shc1, Dok1 (pTyr-361), annexin A2, and enolase.

Also identified ≥4 times from both populations are sites on proteins previously characterized as known or likely Src substrates but for which published evidence is lacking for the specific site(s) being directly targeted by Src, namely, talin-1, GIT1, ZO-1, cofilin-1, Cbl, eEF1A, CDV3A, PI3K p85α, SHP2, and two additional sites on Dok1 (Table 4). Of particular interest in this group are sites on the protein-tyrosine phosphatase SHP2 (pTyr-62) and the p85α regulatory subunit of PI3K (pTyr-467) as they lie in regions involved in regulating enzyme activity. SHP2 exhibits constitutive tyrosine-phosphorylation in Src-transformed cells and has been implicated in morphological transformation.[41,42] Structural studies showed SHP2 Tyr-62 to lie in a region of the N-terminal SH2 domain that inserts into the catalytic cleft to autoinhibit phosphatase activity.[43] PI3K activity is also known to be elevated in Src-transformed cells and implicated in transformation.[44,45] Tyr-467 of the p85α subunit is part of a coiled-coiled domain in the inter-SH2 region that interacts with the p110 catalytic subunit to inhibit activity.[46] Immunoblot analysis using a phosphospecific antibody raised against the p85 pTyr-467 provided further evidence for the elevated phosphorylation of this site in Src-transformed cells (Figure 4C).

Many other sites found ≥4 times from both populations are on proteins not previously implicated as Src substrates. This group includes a predicted protein kinase SgK269 (two sites), a zyxin-family member LPP (lipoma preferred partner, three sites) known to localize to cell/ECM adhesions, actin-associated proteins septin-2 and VASP, small G-protein regulators intersectin-2 and RIN1, a predicted Rho-family GAP that is most closely related to oligophrenin 1, ANKS1/Odin, and the glycolytic enzyme GAPDH (Table 4). VASP Tyr-39 is notable among this group of sites as it is a conserved residue in the EVH1 domain important for subcellular targeting.[47,48] RIN1 Tyr-35 has been previously characterized as a site of phosphorylation by the Abl tyrosine kinase.[49] Immunoblotting with a phosphospecific antibody against RIN Tyr-35 further supports this site as being elevated in the Src-transformed cells (Figure 4D). As Src can act as a positive regulator of Abl by phosphorylating the Abl kinase domain activation loop Tyr-393[50] (in our study, identified 4 times in nontransformed cells and 3 times in Src-transformed cells), it is possible that increased Abl activity contributes to the observed RIN1 Tyr-35 phosphorylation. Other sites presented here as candidate novel Src sites could similarly be targets of other kinases that are activated downstream of Src.

SILAC Analysis of the Impact of Oncogenic Src on the pTyr Proteome

While the spectral-counting analysis revealed much about the striking impact of oncogenic Src on the pTyr proteome, the much greater complexity of the peptide preparations from the Src-transformed cells precluded the use of this approach as a means to provide accurate information on differences between the two cell populations in phosphorylation site stoichiometry. Thus, to complement the spectral counting data, we carried out an independent quantitative comparison using the SILAC method.[51,52] For the SILAC analysis, proteins in the Src-transformed cell population were labeled through six passages in media containing heavy $^{13}C_6$-arginine and $^{13}C_6$-lysine, while the nontransformed cells were maintained in standard growth medium. Then equal numbers of cells from each population were combined prior to cell lysis and subsequent tryptic peptide enrichment through pTyr immunoaffinity purification. Corresponding light and heavy SILAC phopeptides, that co-elute in the reversed-phase step, appear as doublets in MS with the ratio of peak intensities indicating relative differences in phosphorylation stoichiometry (Figure 5, and Supplemental Figure S2). A single round of SILAC analysis was carried out, providing quantitative measures for 48 peptides representing 42 different pTyr sites on 38 different proteins (Supplemental Table S3). Of these 42 sites, 10 were represented by peptides that were clearly detected only as heavy peaks representative of the Src-transformed cell sample.

The SILAC results provided general support for the conclusions made from the label-free spectral count analysis. All but two of the sites identified by SILAC were indicated to have elevated phosphorylation in the Src-transformed cells, with the two exceptions being CDK1 pTyr-15, that was elevated in the nontransformed cells, and GSK3 pTyr-216 that was essentially unchanged (Table 5). In the label-free analysis, these two CMGC kinase sites were among those identified with significantly higher frequency in the nontransformed cells.

Notable among the 40 pTyr sites indicated by SILAC to have elevated phosphorylation in the Src-transformed cells are 11 sites (Table 5) predicted from the label-free analysis as major biologically relevant Src substrates on the basis of their frequent identification in both cell populations. Included are five established Src sites (Src Tyr-418, p190RhoGAP Tyr-943, p130Cas Tyr-253, p120catenin Tyr-96, and enolase Tyr-43) and six of the sites not previously established as Src targets (talin-1 Tyr-26, talin-1 Tyr-70, eEF1A Tyr-29, VASP Tyr-39, RIN-1 Tyr-35, and GAPDH Tyr-315). Thus SILAC provided further evidence in support of these sites being direct targets of oncogenic Src. Of these 11 sites, only enolase Tyr-43 was identified with significantly higher frequency in the Src-transformed cells in the label-free analysis, while the two sites with the lowest heavy/light peak intensity ratios among this group, p190RhoGAP

Tyr-943 (heavy/light) 2.8) and p130Cas Tyr-253 (heavy/light = 4.0), were identified with significantly higher frequency in the nontransformed cells.

A majority of the remaining pTyr sites identified by SILAC as elevated in the Src-transformed cells were on housekeeping proteins including metabolic enzymes and macromolecular synthetic machinery. Thirteen sites identified by SILAC, including enolase Tyr-43 and Src-Tyr-438, were also found in the label-free analysis with significantly higher frequency in the Src-transformed cells and these tended to have higher heavy/light peak intensity ratios. Five sites emerged from the SILAC analysis (on alpha-1 catenin, tight junction protein ZO-1, elongation complex protein 3, DNA damage-binding protein 1, and U1 snRNP 70 kDa; see Supplemental Table S3 for details) that had not been found in the label-free analysis, which is not surprising in light the different instrumentation and set up used in the two approaches.

Conclusions and Prospects

We extensively analyzed the pTyr proteomes of Src-transformed MEFs and counterpart nontransformed cells to provide the most comprehensive view to date of the global impact of oncogenic Src activity on cellular tyrosine phosphorylation. From the two cell populations combined, over 700 distinct pTyr sites were identified. Comparative analysis by spectral counting, an indication of phosphopeptide relative abundance in the sample preparations, revealed profound differences in the two pTyr profiles. While the nontransformed cell pTyr profile was enriched in proteins associated with receptor- and adhesion-associated signaling pathways, the Src-transformed cell profile was distinguished by the large representation of “housekeeping” proteins including many metabolic enzymes and macromolecular synthetic machinery. However, the much greater complexity of the sample preparations from Src-transformed cells, coupled with the sensitivity limitations of data-dependent acquisition in MS, precluded the use of spectral counting as an accurate quantitative measure of differences in phosphorylation stoichiometry between the two cell populations. A complementary analysis using SILAC provided quantitative information on 42 pTyr sites, almost all showing elevated phosphorylation in the Src-transformed cells, generally supporting the conclusions made from the label-free spectral count analysis. On the basis of frequent detection in both the nontransformed and Src-transformed cell populations, a subset of 43 pTyr sites (representing 32 proteins) were predicted as major biologically relevant Src targets with elevated phosphorylation in the Src-transformed cells. This select group, of particular interest for biomarker monitoring of Src activity in biological samples including cancers, includes many well-established Src sites on signaling, adhesion, and cytoskeletal proteins but also several previously uncharacterized sites on regulatory domains of signaling proteins relevant to the transformed phenotype. Eleven of these sites, including six not previously establish as Src targets, were further indicated by SILAC to have elevated phosphorylation in the Src-transformed cells. It will be important to validate the candidate novel Src sites as being *bona fide* Src sites, or targets of other kinases activated downstream of Src, through additional experimentation such as *in vitro* kinase assays and *in vivo* kinetic analysis after treatment with Src-selective inhibitors. Also of interest for future studies will be to evaluate these sites in epithelial-derived carcinomas for potential usefulness in cancer treatment as tumor biomarkers of elevated Src activity and *in vivo* responsiveness to therapeutic Src-inhibition.

Supplementary Material

Refer to Web version on PubMed Central for supplementary material.

Abbreviations

LC-MS/MS, liquid chromatography-tandem mass spectrometry; MEF, mouse embryo fibroblast; pTyr, phosphotyrosine; SILAC, stable isotope labeling with amino acids in cell culture.

Acknowledgment

We thank Larisa Ryzhova and Kristen Cheek for technical assistance, John Colicelli for generously providing RIN1 antibodies, and Bob Coffey and Tony Hunter for encouragement and helpful comments. Supported by NIH grants GM49882 (S.K.H.), CA106424 (A.P.), U54 RR020839 (A.P.), Vanderbilt GI-SPORE grant NCI 2P50 CA95103, and Vanderbilt-Ingram Cancer Center support grant CA68485.

References

1. Hunter T, Sefton BM. Transforming gene product of Rous sarcoma virus phosphorylates tyrosine. Proc. Natl. Acad. Sci. U.S.A 1980;77:1311–1315. [PubMed: 6246487]
2. Jove R, Hanafusa H. Cell transformation by the viral src oncogene. Ann. Rev. Cell Biol 1987;3:31–56. [PubMed: 2446642]
3. Frame MC. Newest findings on the oldest oncogene; how activated src does it. J. Cell Sci 2004;117:989–998. [PubMed: 14996930]
4. Summy JM, Gallick GE. Src family kinases in tumor progression and metastasis. Cancer Metastasis Rev 2003;22:337–358. [PubMed: 12884910]
5. Yeatman TJ. A renaissance for SRC. Nat. Rev. Cancer 2004;4:470–480. [PubMed: 15170449]
6. Mitra SK, Schlaepfer DD. Integrin-regulated FAK-Src signaling in normal and cancer cells. Curr. Opin. Cell Biol 2006;18:516–523. [PubMed: 16919435]
7. Bromann PA, Korkaya H, Courtneidge SA. The interplay between Src family kinases and receptor tyrosine kinases. Oncogene 2004;23:7957–7968. [PubMed: 15489913]
8. Ishizawar R, Parsons SJ. c-Src and cooperating partners in human cancer. Cancer Cell 2004;6:209–214. [PubMed: 15380511]
9. Luttrell DK, Luttrell LM. Not so strange bedfellows: G-protein-coupled receptors and Src family kinases. Oncogene 2004;23:7969–7978. [PubMed: 15489914]
10. Thomas SM, Brugge JS. Cellular functions regulated by Src family kinases. Ann. Rev. Cell Dev. Biol 1997;13:513–609. [PubMed: 9442882]
11. Martin GS. The hunting of the Src. Nat. Rev. Mol. Cell. Biol 2001;2:467–475. [PubMed: 11389470]
12. Rush J, Moritz A, Lee KA, Guo A, Goss VL, Spek EJ, Zhang H, Zha XM, Polakiewicz RD, Comb MJ. Immunoaffinity profiling of tyrosine phosphorylation in cancer cells. Nat. Biotechnol 2005;23:94–101. [PubMed: 15592455]
13. Brábek J, Constancio SS, Shin NY, Pozzi A, Weaver AM, Hanks SK. CAS promotes invasiveness of Src-transformed cells. Oncogene 2004;23:7406–7415. [PubMed: 15273716]
14. Cortes HJ, Pfeiffer C, Richter B, Stevens T. Porous ceramic bed supports for fused-silica packed capillary columns used in liquid-chromatography. High Resol. Chromatogr. Chromatogr. Commun 1987;10:446–448.
15. Licklider LJ, Thoreen CC, Peng J, Gygi SP. Automation of nanoscale microcapillary liquid chromatography-tandem mass spectromentry with a vented column. Anal. Chem 2002;74:3076–3083. [PubMed: 12141667]
16. Yates JR III, Eng JK, McConnack AL, Schieltz D. Method to correlate tandem mass-spectra of modified peptides to aminoacid-sequences in the protein database. Anal. Chem 1995;67:1426–1436. [PubMed: 7741214]
17. Gao J, Opiteck GJ, Friedrichs MS, Dongre AR, Hefta SA. Changes in the protein expression of yeast as a function of carbon source. J. Proteome Res 2003;2:643–649. [PubMed: 14692458]
18. Amanchy R, Kalume DE, Pandey A. Stable isotope labeling with amino acids in cell culture (SILAC) for studying dynamics of protein abundance and posttranslational modifications. Sci. STKE 2005;18:l2.

19. Andersen JS, Wilkinson CJ, Mayor T, Mortensen P, Nigg EA, Mann M. Proteomic characterization of the human centrosome by protein correlation profiling. Nature 2003;426:570–574. [PubMed: 14654843]
20. Brábek J, Constancio SS, Siesser PF, Shin NY, Pozzi A, Hanks SK. Crk-associated substrate tyrosine phosphorylation sites are critical for invasion and metastasis of Src-transformed cells. Mol. Cancer Res 2005;3:307–315. [PubMed: 15972849]
21. Gould KL, Nurse P. Tyrosine phosphorylation of the fission yeast cdc2 + protein kinase regulates entry into mitosis. Nature 1989;342:39–45. [PubMed: 2682257]
22. Cooper JA, Reiss NA, Schwartz RJ, Hunter T. Three glycolytic enzymes are phosphorylated at tyrosine in cells transformed by Rous sarcoma virus. Nature 1983;302:218–223. [PubMed: 6188054]
23. Manning G, Whyte DB, Martinez R, Hunter T, Sudarsanam S. The protein kinase complement of the human genome. Science 2002;298:1912–1934. [PubMed: 12471243]
24. Lochhead PA, Kinstrie R, Sibbet G, Rawjee T, Morrice N, Cleghon V. A chaperone-dependent GSK3β transitional intermediate mediates activation-loop autophosphorylation. Mol. Cell 2006;24:627–633. [PubMed: 17188038]
25. Lochhead PA, Sibbet G, Morrice N, Cleghon V. Activation-loop autophosphorylation is mediated by a novel transitional intermediate form of DYRKs. Cell 2005;121:925–936. [PubMed: 15960979]
26. Hanks SK, Ryzhova L, Shin NY, Brábek J. Focal adhesion kinase signaling activities and their implications in the control of cell survival and motility. Front. Biosci 2003;8:d982–d996. [PubMed: 12700132]
27. Arthur WT, Petch LA, Burridge K. Integrin engagement suppresses RhoA activity via a c-Src-dependent mechanism. Curr. Biol 2000;10:719–722. [PubMed: 10873807]
28. Zeng L, Si X, Yu WP, Le HT, Ng KP, Teng RMH, Ryan K, Wang DZM, Ponniah S, Pallen CJ. PTPα regulates integrin-stimulated FAK autophosphorylation and cytoskeletal rearrangement in cell spreading and migration. J. Cell Biol 2003;160:137–146. [PubMed: 12515828]
29. Galisteo ML, Yang Y, Ureña J, Schlessinger J. Activation of the nonreceptor protein tyrosine kinase Ack by multiple extracellular stimuli. Proc. Natl. Acad. Sci. U.S.A 2006;103:9796–9801. [PubMed: 16777958]
30. Kullander K, Klein R. Mechanisms and functions of Eph and ephrin signalling. Nat. Rev. Mol. Cell. Biol 2002;3:475–486. [PubMed: 12094214]
31. Noguchi T, Matozaki T, Inagaki K, Tsuda M, Fukunaga K, Kitamura Y, Kitamura T, Shii K, Yamanashi Y, Kasuga M. Tyrosine phosphorylation of p62Dok induced by cell adhesion and insulin: possible role in cell migration. EMBO J 1999;18:1748–1760. [PubMed: 10202139]
32. Woodring PJ, Meisenhelder J, Johnson SA, Zhou GL, Field J, Shah K, Bladt F, Pawson T, Niki M, Pandolfi PP, Wang JYJ, Hunter T. c-Abl phosphorylates Dok1 to promote filopodia during cell spreading. J. Cell Biol 2004;165:493–503. [PubMed: 15148308]
33. Yu H, Rosen MK, Shin TB, Seidel-Dugan C, Brugge Js, Schreiber SL. Solution structure of the SH3 domain of Src and identification of its ligand-binding site. Science 1992;258:1665–1668. [PubMed: 1280858]
34. Weijland A, Neubauer G, Courtneidge SA, Mann M, Wierenga RK, Superti-Furga G. The purification and characterization of the catalytic domain of src expressed in *Schizosaccharomyces pombe*. Eur. J. Biochem 1996;240:756–764. [PubMed: 8856081]
35. Gerke V. Tyrosine protein kinase substrate p36: A member of the annexin family of Ca2+/phospholipid-binding proteins. Cell Motil. Cytoskeleton 1989;14:449–454. [PubMed: 2533882]
36. Sefton BM, Hunter T, Ball EH, Singer SJ. Vinculin: a cytoskeletal target of the transforming protein of rous sarcoma virus. Cell 1981;24:165–174. [PubMed: 6263485]
37. Christofk HR, Vander Heiden MG, Wu N, Asara JM, Cantley LC. Pyruvate kinase M2 is a phosphotyrosine binding protein. Nature 2008;452:181–186. [PubMed: 18337815]
38. Christofk HR, Vander Heiden MG, Harris MH, Ramanathan A, Gerszten RE, Wei R, Fleming MD, Schreiber SL, Cantley LC. The M2 splice isoform of pyruvate kinase is important for cancer metabolism and tumour growth. Nature 2008;452:230–233. [PubMed: 18337823]
39. Reiss N, Kanety H, Schlessinger J. Five enzymes of the glycolytic pathway serve as substrates for purified epidermal-growth-factor kinase. Biochem. J 1986;239:691–697. [PubMed: 3030270]

40. Gondran P, Dautry F. Regulation of mRNA splicing and transport by the tyrosine kinase activity of src. Oncogene 1999;18:2547–2555. [PubMed: 10353598]
41. Feng GS, Hui CC, Pawson T. SH2-containing phosphotyrosine phosphatase as a target of protein-tyrosine kinases. Science 1993;259:1607–1611. [PubMed: 8096088]
42. Hakak Y, Hsu YS, Martin GS. Shp-2 mediates v-Src-induced morphological changes and activation of the anti-apoptotic protein kinase Akt. Oncogene 2000;19:3164–3171. [PubMed: 10918571]
43. Hof P, Pluskey S, Dhe-Paganon S, Eck MJ, Shoelson SE. Crystal structure of the tyrosine phosphatase SHP-2. Cell 1998;92:441–450. [PubMed: 9491886]
44. Whitman M, Downes CP, Keeler M, Keller T, Cantley L. Type I phosphatidylinositol kinase makes a novel inositol phospholipid, phosphatidylinositol-3-phosphate. Nature 1988;332:644–646. [PubMed: 2833705]
45. Penuel E, Martin GS. Transformation by v-Src: Ras-MAPK and PI3K-mTOR mediate parallel pathways. Mol. Biol. Cell 1999;10:1693–1703. [PubMed: 10359590]
46. Dhand R, Hara K, Hiles I, Bax B, Gout I, Panayotou G, Fry MJ, Yonezawa K, Kasuga M, Waterfield MD. PI 3-kinase: structural and functional analysis of intersubunit interactions. EMBO J 1994;13:511–521. [PubMed: 8313896]
47. Gertler FB, Niebuhr K, Reinhard M, Wehland J, Soriano P. Mena, a relative of VASP and Drosophila Enabled, is implicated in the control of microfilament dynamics. Cell 1996;87:227–239. [PubMed: 8861907]
48. Krause M, Leslie JD, Stewart M, Lafuente EM, Valderrama F, Jagannathan R, Strasser GA, Rubinson DA, Liu H, Way M, Yaffe MB, Boussiotis VA, Gertler FB. Lamellipodin, an Ena/VASP ligand, is implicated in the regulation of lamellipodial dynamics. Dev. Cell 2004;7:571–583. [PubMed: 15469845]
49. Hu H, Bliss JM, Wang Y, Colicelli J. RIN1 Is an ABL tyrosine kinase activator and a regulator of epithelial-cell adhesion and migration. Curr. Biol 2005;15:815–823. [PubMed: 15886098]
50. Plattner R, Kadlec L, DeMali KA, Kazlauskas A, Pendergast AM. c-Abl is activated by growth factors and Src family kinases and has a role in the cellular response to PDGF. Genes Dev 1999;13:2400–2411. [PubMed: 10500097]
51. Molina H, Parmigiani G, Pandey A. Assessing reproducibility of a protein dynamics study using in vivo labeling and liquid chromatography tandem mass spectrometry. Anal. Chem 2005;77:2739–2744. [PubMed: 15859588]
52. Ibarrola N, Kalume DE, Gronborg M, Iwahori A, Pandey A. A proteomic approach for quantitation of phosphorylation using stable isotope labeling in cell culture. Anal. Chem 2003;75:6043–6049. [PubMed: 14615979]

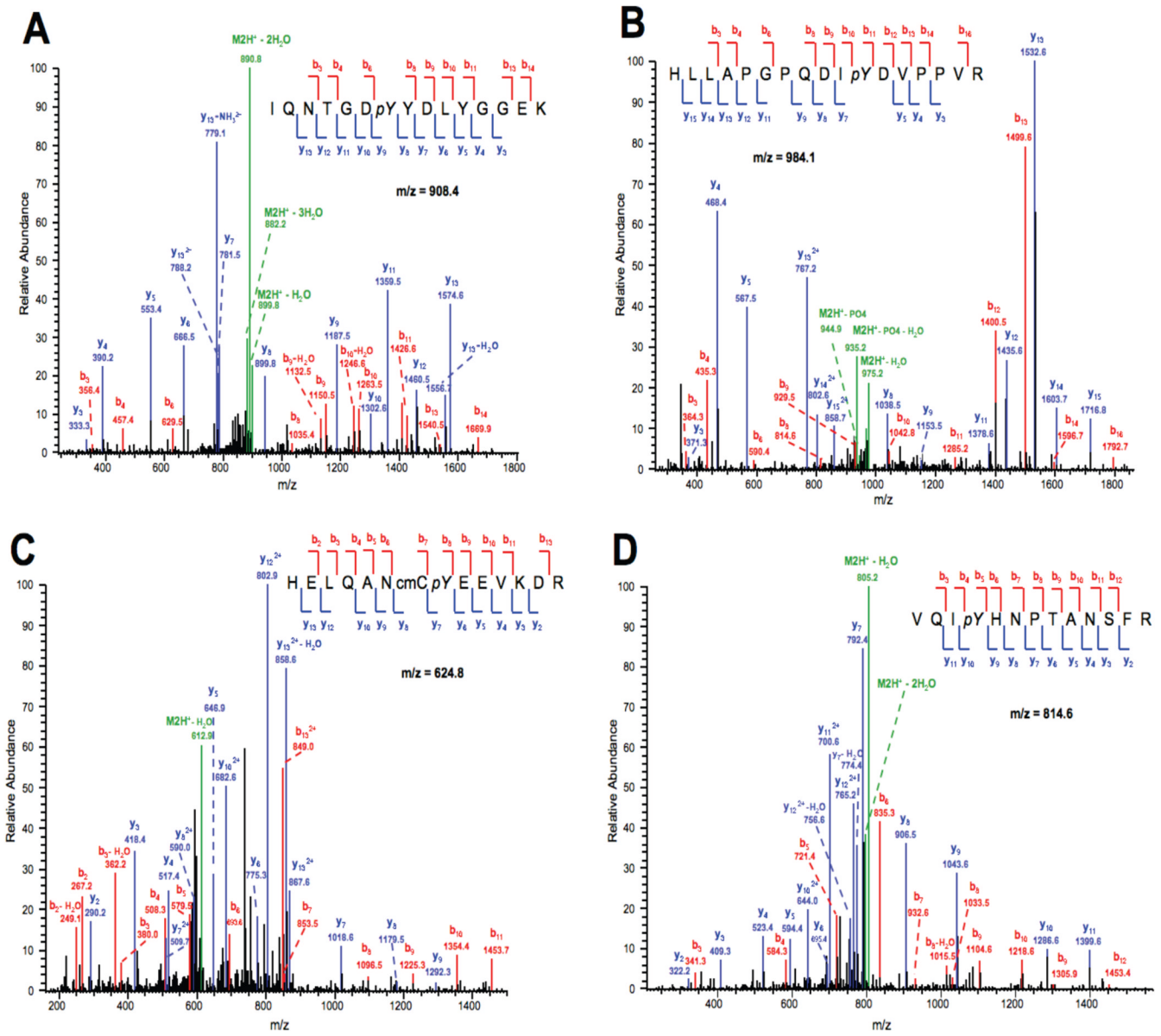

Figure 1.

Representative MS/MS spectra for pTyr-containing peptides. The spectra shown are from four different pTyr-containing tryptic peptides that were readily detected in both the Src-transformed and nontransformed cell populations: (A) doubly-charged tryptic peptide from tyrosine phosphatase SHP-2 pTyr-62, (B) doubly-charged tryptic peptide from p130Cas pTyr-253, (C) triply-charged tryptic peptide from cofilin-1 pTyr-139, and (D) doubly-charged tryptic peptide from VASP pTyr-39. The precursor *m/z* values for each spectrum are indicated on each panel. In the peptide sequences, *pY* indicates phosphotyrosine, while “cmC” in the cofilin-1 peptide indicates a carboxyamidomethylated cysteine.

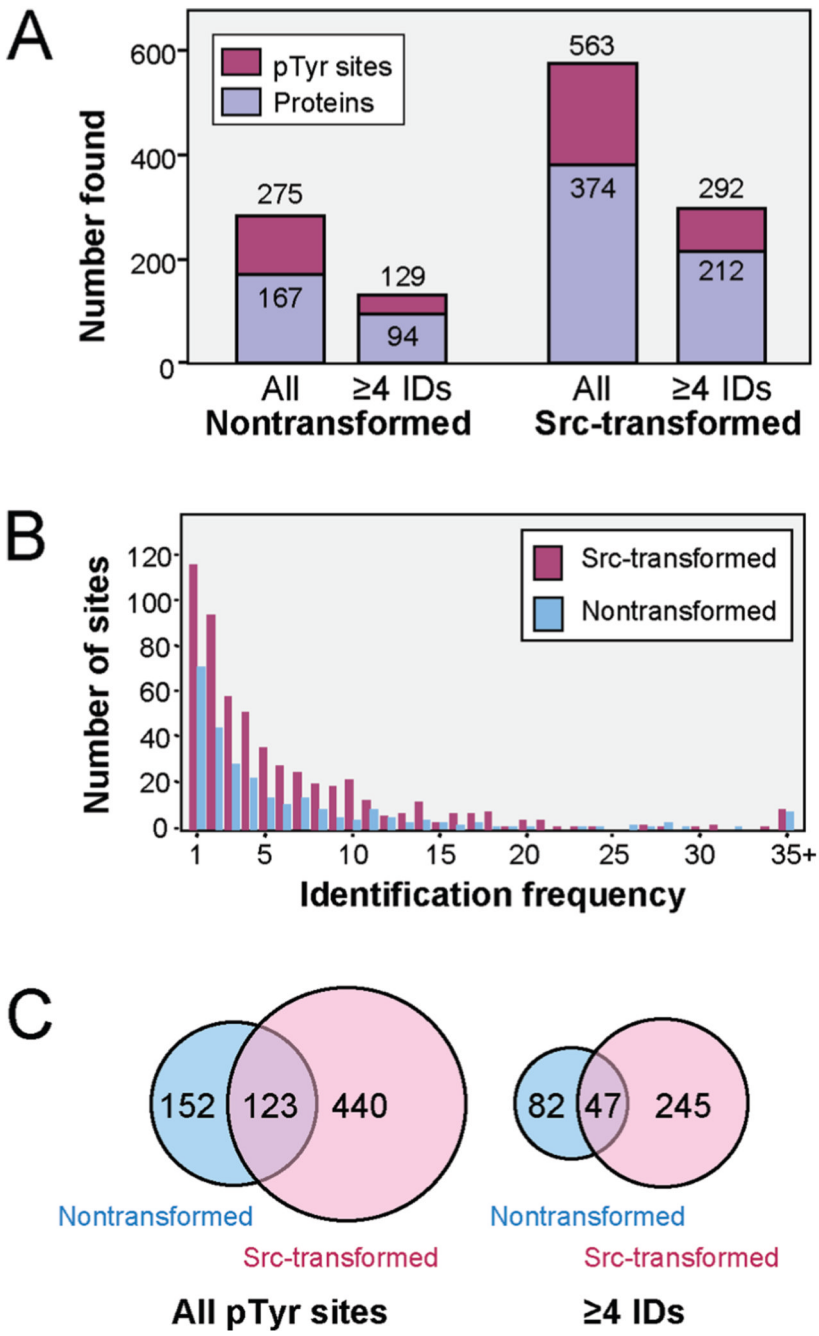

Figure 2.

Overview of the pTyr profiles. (A) Totals of pTyr sites and represented proteins from the nontransformed vs Src-transformed cell populations, considering either all retained sites (All) or only sites with at least 4 independent identifications (≥4 IDs). (B) Identification frequencies of retained pTyr sites reflects a Poisson distribution. (C) Venn diagrams depicting pTyr sites identified uniquely in each cell population and common to both. Left, all retained sites (715 total). Right, sites with ≥4 identifications (374 total).

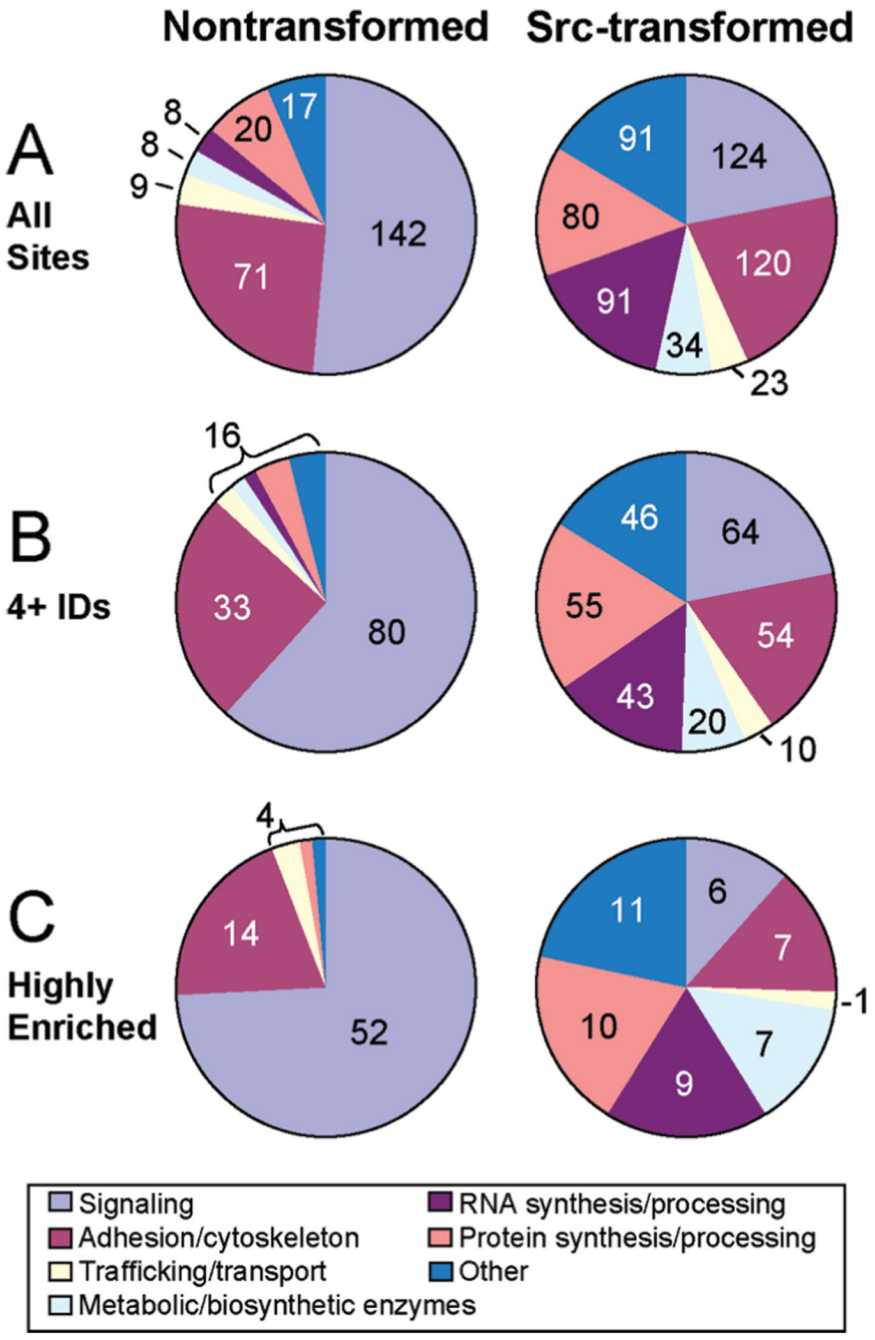

Figure 3.

Protein functional classes represented in the profiles. The pie-charts show distributions of pTyr sites from nontransformed (left) and Src-transformed (right) cells according to a broad functional classification of represented proteins. Color-coding is according to the functional categories shown at bottom, with numbers indicating distinct sites within each. (A) All retained sites. (B) Sites with ≥4 identifications. (C) Sites "highly-enriched" in one cell population vs the other based on peptide frequency-based analysis.

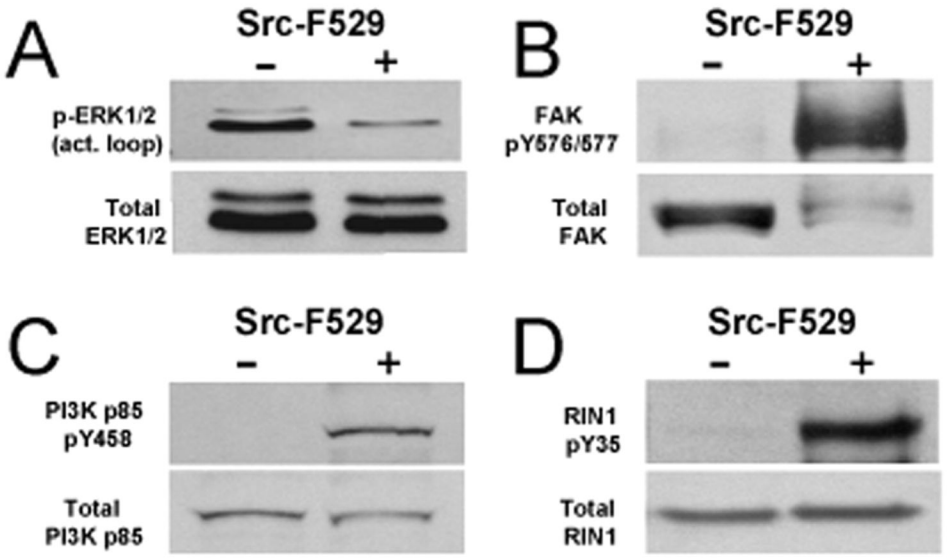

Figure 4.
Immunoblot analyses of representative pTyr sites. Total cell lysates (30 μg protein/lane) were analyzed using phosphospecific antibodies as indicated.

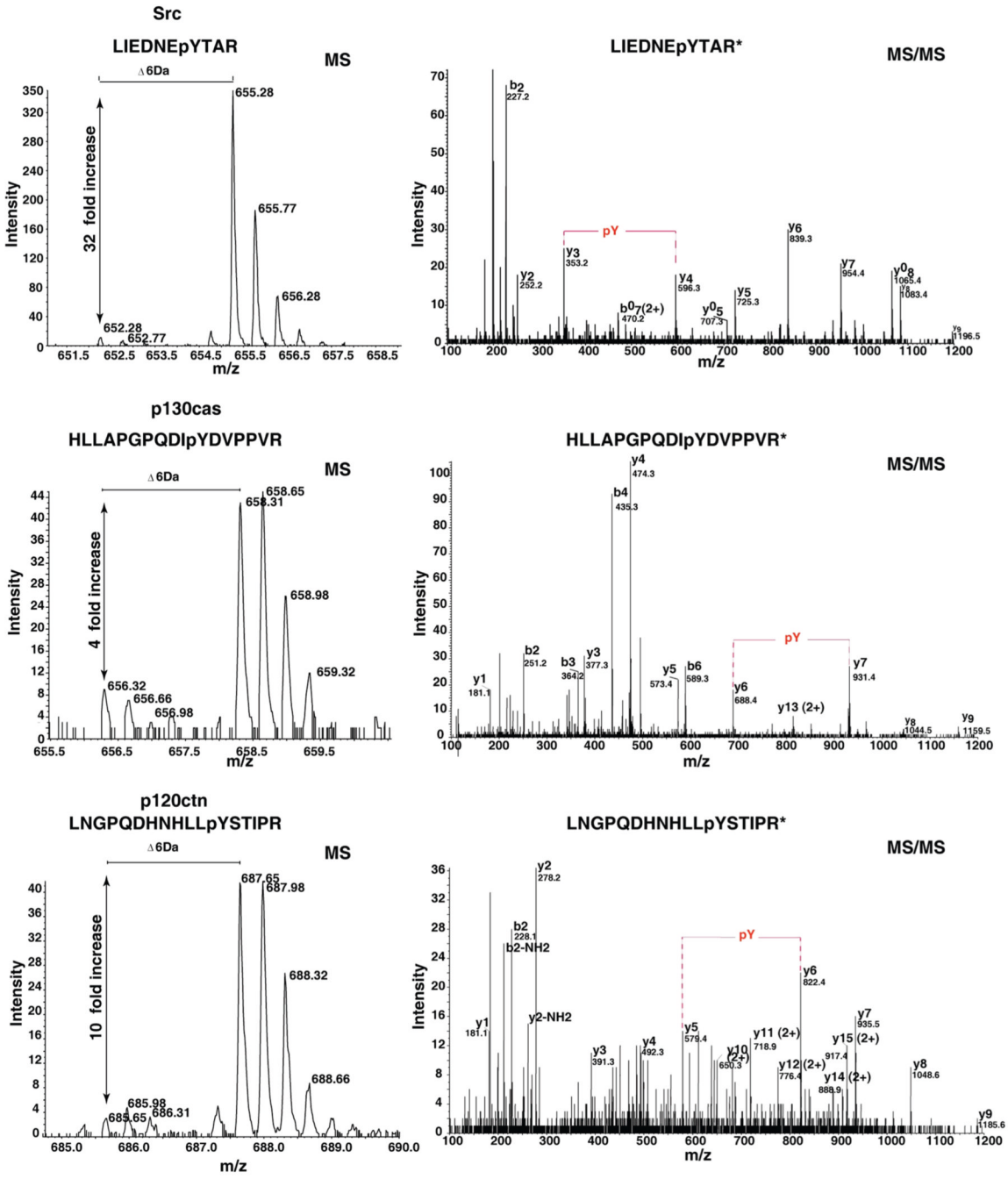

Figure 5.

Examples of quantitation by SILAC. The panels show the MS and MS/MS spectra of three different pTyr-containing peptides. MS spectra show the fold changes in the level of heavy labeled peptide (from Src-transformed cells) versus light peptide (from nontransformed cells). MS/MS spectra shows the annotation of fragment ions (b and y ions) of the more intense heavy peptide peak, confirming the sequence and phosphorylation sites (*pY*). Asterisk (*) represents the $^{13}C_6$-labeled amino acid (R/K). Top, MS and corresponding MS/MS spectra of peptide LIEDNE*pY*TAR from Src (pTyr-418). Middle, MS and corresponding MS/MS spectra of peptide NEEENI*pY*SVPHDSTQGK from p190RhoGAP (pTyr-943). Bottom, MS and

corresponding MS/MS spectra of peptide HLLAPGPQDI*pY*DVPPVR from p130Cas (pTyr-253).

Table 1
Ten Most Frequently Identified Sites

protein	site[a]	IDs
	Nontransformed Cells	
CDK1	Y15	132
GSK3β	*Y216	92
FAK	*Y576	73
ERK2	*Y185	63
Dok1	Y361	54
Paxillin	Y118	50
p38α MAPK	*Y181	47
PRP4	*Y849	46
p130Cas	Y253	32
DYRK1A	*Y145	29
	Src-Transformed Cells	
Enolase α	Y24	100
hnRNP Q	Y485	85
Enolase α	Y43	81
PSMA2	Y75	72
PSMA2	Y100	45
GAPDH	Y315	41
DDX3X	Y461	40
GIT1	Y554	40
Src	Y92	37
Dok1	Y361	34

[a] Asterisks (*) indicate activation loop site in protein kinase domain.

Table 2

Sites Detected with Significantly Higher Frequency in the Nontransformed Cell Population[a]

	ID #	Protein Name	Site	Representative peptide	Nontransformed cells: trypsin 1 2 3 4 5 6 7 8 9 10	Nontransformed cells: chymotrypsin 11 12 13 14 15 16 17 18	Src-transformed cells: trypsin 1 2 3 4 5 6 7 8 9 10	Src-transformed cells: chymotrypsin 11 12 13 14 15 16 17 18
Signaling: Tyrosine kinases	Q80XU2	Src	Y529	F.LEDYFTSTEPQY@QPGENL.-	0 0 0 0 0 0 0 0 0 0	2 2 2 1 1 1 0 1	0 0 0 0 0 0 0 0 0 0	0 0 0 0 0 0 0 0 0 0
	P39688	Fyn (Yes)	Y527	F.LEDYFTATEPQY@QPGENL.-	0 0 0 0 0 0 0 0 0 0	0 1 1 1 0 0 1 0 1 1	0 0 0 0 0 0 0 0 0 0	0 0 0 0 0 0 0 0 0 0
	Q922K9	Frk	Y504	W.KLEDYFETDC*SY@SDTNNFIN.-	0 0 0 0 0 0 0 0 0 1	0 3 0 1 0 2 1 0 2 1	0 0 0 0 0 0 0 0 0 0	0 0 0 0 0 0 0 0 0 0
	P70451	Fer	Y402	K.VQENDGKEPPPVVNY@EEDAR.S	1 2 4 4 0 1 1 2 1 0	0 0 0 0 0 0 0 0 0 0	0 0 1 0 0 0 0 0 0 0	0 0 0 0 0 0 0 0 0 0
	P34152-3	FAK	Y397	M.RTHAVSVSETDDY@AEIIDEEDTY.T	0 0 0 2 0 0 1 0 0 0	5 2 0 0 0 0 0 1	0 0 0 0 0 0 0 0 0 0	0 0 0 0 0 0 0 0 0 0
	P34152-3	FAK	***Y576***	R.YM#EDSTY@YK.A	4 7 6 4 3 7 5 10 6 1	4 1 2 0 4 4 0 5	0 2 2 0 1 2 2 2 3 3	0 0 0 0 0 0 0 0 0 0
	P34152-3	FAK	***Y577***	R.YM#EDSTY@Y@K.A	0 2 2 1 1 3 1 6 4 1	1 0 1 0 2 1 0 1	0 0 0 0 0 0 0 2 2 2	0 0 0 0 0 0 0 0 0 0
	O54967	ACK	Y874	K.VSSTHY@YLLPERPPYLER.Y	0 1 0 2 1 0 1 1 1 1	0 0 0 0 0 0 0 0	0 0 0 0 0 0 0 0 0 0	0 0 0 0 0 0 0 0 0 0
	O54967-2	ACK, splice isoforms 2 and 3	Y518	R.VKKPTY@DPVSEDPDPLSSDFKR.L	1 1 3 4 0 1 0 2 0 1	0 1 1 0 0 2 2 0	0 0 0 0 0 0 0 0 0 0	0 0 0 0 0 0 0 0 0 0
	Q00993	Axl	***Y696***	K.IYNGDY@YR.Q	2 1 3 4 2 2 2 2 2 2	1 1 0 0 0 0 0 0	0 1 1 0 0 0 0 1	0 0 0 0 0 0 0 0
	Q62371	DDR2	***Y481***	R.IFPLRPDY@QEPSR.L	0 1 1 1 0 0 0 0 0 0	1 0 1 0 0 0 0 0	0 0 0 0 0 0 0 0 0 0	0 0 0 0 0 0 0 0 0 0
	Q03145	EphA2	Y589	L.KTY@VDPHTY@EDPNQAVL.K	0 0 0 0 0 0 1 0 0 0	0 2 1 1 0 1 0 0	0 0 0 0 0 0 0 0 0 0	0 0 0 0 0 0 0 0 0 0
	Q03145	EphA2	Y595	K.SEQLKPLKT@YVDPHTY@EDPNQAVLK.F	3 2 1 2 1 1 2 2 2 3	1 1 1 1 1 1 0 1	1 0 0 0 0 0 0 0 0 0	0 0 0 0 0 0 0 0 0 0
	Q03145	EphA2	***Y773***	R.VLEDDPEATY@TTSGGKIPIR.W	1 3 2 2 0 2 1 2 1 1	1 2 1 1 1 1 0 1	0 0 0 0 0 0 0 0 0 1	0 0 0 0 0 0 0 0 0 0
	P54754	EphB3 (EphB4)	Y603	K.VY@IDPFTY@EDPNEAVR.E	0 0 0 0 5 0 0 0 0 0	0 0 0 0 0 0 0 0	0 0 0 0 0 0 0 0 0 0	0 0 0 0 0 0 0 0 0 0
	P54754	EphB3 (EphB4)	Y609	K.VYIDPFTY@EDPNEAVR.E	0 1 0 1 5 1 1 1 1 1	0 0 0 0 0 0 0 0	0 0 0 0 0 0 0 0 0 0	0 0 0 0 0 0 0 0 0 0
	Q60751	IGF1R (InsR)	***Y1167***	R.DIYETDY@YR.K	0 1 1 0 0 1 0 3 0 1	0 0 0 0 0 0 0 0	0 0 0 0 0 0 0 0 0 0	0 0 0 0 0 0 0 0 0 0
	P16056	MET	***Y1232***	R.DMYDKEY@YSVHNK.T	2 1 4 2 1 2 1 6 4 2	0 0 0 0 1 0 0 0	0 0 0 0 0 0 0 0 0 0	0 0 0 0 0 0 0 0 0 0
	P16056	MET	***Y1233***	R.DMYDKEY@YQSVHNK.T	1 0 3 0 0 0 1 4 2 1	0 1 0 0 0 0 0 0	1 0 0 0 0 0 0 0 0 0	0 0 0 0 0 0 0 0 0 0
Signaling: CMGC kinases	P11440	CDK1 (CDK2)	Y15	K.IGEGTY@GVVYK.G	7 11 15 21 10 16 11 10 7 8	4 2 2 1 2 3 0 2	1 1 1 1 0 0 2 1 1 1	0 0 0 0 0 0 0 0 0 0
	Q63844	ERK1	***Y205***	R.IADPEHDHTGFLTEY@VATR.W	2 2 2 2 1 0 2 3 1 3	5 3 2 0 0 0 0 0	0 0 0 0 0 0 0 0 0 0	0 0 0 0 0 0 0 0 0 0
	P63085	ERK2	***Y185***	R.VADPDHDHTGFLTEY@VATR.W	8 4 2 7 3 2 6 6 5 3	4 5 4 3 0 1 0 0	0 0 0 0 0 0 0 0 0 0	0 0 0 0 0 0 0 0 0 0
	Q9WVS8	ERK5	***Y221***	R.GLC*TSPAEHQYFMTEY@VATR.W	1 1 0 3 0 1 0 0 1 0	0 0 0 0 0 0 0 0	0 0 0 0 0 0 0 0 0 0	0 0 0 0 0 0 0 0 0 0
	P47811	p38alpha	***Y181***	R.HTDDEMTGY@VATR.W	3 4 4 3 0 3 2 2 1 1	9 5 4 1 2 1 0 2	0 0 0 0 0 0 0 0 0 0	0 0 0 0 0 0 0 0 0 0
	Q9WV60	GSK3b (GSK-3a)	***Y216***	L.VRGEPNVSY@IC*SRY.Y	3 2 3 2 2 3 1 3 4 2	20 12 7 4 9 5 5 5	0 0 1 0 0 0 1 0	0 1 1 0 0 0 0 1
	Q61214	DYRK1A	Y145	R.KVYNDGYDDDNY@DYIVK.N	2 3 3 4 0 3 2 3 2 1	2 0 1 0 2 1 0 0	0 0 0 0 1 2 1 0	1 0 0 0 1 1 1 0
	Q61214	DYRK1A (DYRK1B)	***Y321***	R.IYQY@IQSR.F	1 1 1 2 0 1 1 0 1 1	0 1 0 0 1 0 0 0	1 0 0 0 0 0 0 0 0 0	0 0 0 0 0 0 0 0 0 0
	O88904	HIPK1 (HIPK2)	***Y352***	K.AVC*STY@LQSR.Y	1 1 2 2 1 1 0 1 1 0	2 3 2 0 0 0 0 0	0 0 0 0 0 0 0 0 0 0	0 0 0 0 0 0 0 0 0 0
	Q9ERH7	HIPK3	***Y359***	K.TVC*STY@LQSR.Y	1 1 1 1 0 1 0 1 0 0	2 1 1 0 0 0 0 0	0 0 0 0 0 0 0 0 0 0	0 0 0 0 0 0 0 0 0 0
	Q61136	PRP4	***Y849***	K.LC*DFGSASHVADNDITPY@LVSR.F	3 4 2 4 3 3 2 2 2 2	3 2 3 2 3 4 0 2	1 1 1 0 0 1 0 0	1 0 0 0 1 0 0 0
Other Signaling	P52800	Ephrin-B2 (Ephrin-B1)	Y333	K.VSGDYGHPVYIVQEMPPQSPANIY@YKV.-	1 2 2 6 0 0 1 0 1 1	0 0 0 0 0 0 0 0	0 0 0 0 0 0 0 0 0 0	0 0 0 0 0 0 0 0 0 0
	P18052	R-PTPalpha	Y825	K.VVQEYIDAFSDY@ANFK.-	3 2 3 2 1 0 2 0 1 2	5 1 2 0 1 1 0 2	0 0 0 0 0 0 0 0 0 0	0 0 0 0 0 0 0 0 0 0
	Q91YM2	p190RhoGAP	Y943	R.NEEENIY@SVPHDSTQGK.I	2 3 2 7 2 2 3 3 2 2	0 0 0 0 0 0 0 0	2 3 2 3 1 2 2 1 2 2	0 0 0 0 0 0 0 0 0 0
	Q9JLQ2	RhoGAP-12	Y241	K.QNSTPESDY@DNTAC*DPEPDDTGSTR.K	0 1 2 3 0 1 1 1 1 1	0 0 1 0 1 1 0 0	0 1 0 1 0 0 0 0	1 0 0 0 0 0 0 0
	Q9QZK2	BCAR3	Y103	R.KGENFIFRDPY@LLDPTLEYVK.F	0 1 0 2 1 0 1 0 0 0	2 0 0 0 0 0 0 0	0 0 0 0 0 0 0 0	0 0 0 0 0 0 0 0
	Q8CBW3	Abl interactor 1 - Abi-1	Y212	K.TLEPVKPPTVPNDY@MTSPAR.L	0 1 0 3 0 0 1 0 0 0	0 1 1 0 0 0 0 0	0 0 0 0 0 0 0 0	0 0 0 0 0 0 0 0
	P62204	Calmodulin	Y99	R.VFDKDGNGY@ISAAELR.H	0 1 2 2 0 0 0 0 0 0	1 0 0 0 0 0 0 0	0 0 0 0 0 0 0 0	0 0 0 0 0 0 0 0
	Q9WVC3	Caveolin-2	Y27	F.MADDAYS@HHS@GVDY@ADPEKY.V	0 0 0 0 0 0 0 0 0 0	5 3 0 0 1 1 0 0	0 0 0 0 0 0 0 0	0 0 0 0 0 0 0 0
	P47941	Crk-like protein - CrkL	Y198	H.GNRNS@NSY@GIPEPAHAY.A	0 0 1 1 0 0 1 0 0 0	2 1 2 0 0 0 0 0	0 0 0 0 0 0 0 0	0 0 0 0 0 0 0 0
	P47941	Crk-like protein - CrkL	Y207	R.NSNSYGIPEPAHAY@AQPQTTTPLPTVASTPGAAI NPLPSTQNGPVFAK.A	1 2 0 0 1 0 0 0 1 0	0 0 0 0 0 0 0 0	0 0 0 0 0 0 0 0	0 0 0 0 0 0 0 0
	P97465	Docking-protein-1 - Dok1	Y361	K.TKLTDSKEDPIY@DEPEGLAPAPPR.G	3 5 5 5 2 4 4 5 5 4	3 1 2 1 2 1 1 1	5 5 5 4 4 2 1 2 1 2	1 1 0 0 0 0 0 1
	Q9QYY0	Gab1	Y407	K.DASSQDC*Y@DIPR.T	2 2 3 3 1 1 0 1 1 0	2 0 1 0 0 0 0 0	0 0 0 0 0 0 0 0	0 0 0 0 0 0 0 0
	Q3U2I0	IRS-2 (4PS)	Y754	R.SYKAPC*SC*SGDDDQY@VLMSSPVGR.I	1 1 1 1 0 1 1 0 0 0	0 0 0 0 0 0 0 0	0 0 0 0 0 0 0 0	0 0 0 0 0 0 0 0
	Q80TH2	Protein LAP2	Y1097	R.RTEGDY@LSYR.E	1 2 2 2 1 2 0 1 2 0	0 0 0 0 0 0 0 0	0 0 0 0 0 0 0 0	0 0 0 0 0 0 0 0
	Q3TEW6	myelin protein zero-like 1 - PZR	Y264	K.INKSESVVY@ADIR.K	0 2 5 1 0 0 0 0 0 0	2 1 0 0 0 0 0 0	0 0 0 0 0 0 0 0	0 0 0 0 0 0 0 0
	Q6PD21	adapter protein - Shb	Y113	C.RLDY@C*GGGGGGDPGGGQRAF.T	0 0 0 0 1 1 0 1 1 0	2 3 0 0 2 0 0 0	0 0 0 0 0 0 0 0	0 0 0 0 0 0 0 0
	Q6PD21	adapter protein - Shb	Y240	K.DKVTIADDY@SDPFDAK.S	0 0 3 3 0 2 1 3 1 0	1 0 0 0 0 1 0 1	0 0 0 0 0 0 0 0	0 0 0 0 0 0 0 0
	Q6PD21	adapter protein - Shb	Y262	K.AGKGESAGY@MEPYEAQR.I	1 2 3 3 0 0 0 2 0 1	3 0 0 0 0 0 0 0	0 0 0 0 0 0 0 0	0 0 0 0 0 0 0 0
	Q6PD21	adapter protein - Shb	Y330	R.ESKLPQDDDRPADEY@DQPWEWNR.V	0 2 2 2 0 0 0 1 1 0	1 0 1 0 0 0 0 0	0 0 0 0 0 0 0 0	0 0 0 0 0 0 0 0
	P98083	SHC1	Y423	R.ELFDDPSY@VNIQNLDK.A	4 1 4 2 1 2 1 1 3 1	0 0 0 0 0 0 0 0	1 1 1 1 0 1 1 0	1 1 0 0 0 0 0 0
	P42227	STAT3	Y705	K.YC*RPESQEHPEADPGSAAPY@LK.T	1 2 1 1 0 1 1 1 1 1	0 0 0 0 0 0 0 0	0 0 0 0 0 0 1 0	0 0 0 0 0 0 0 0
	P42227-3	STAT3 splice isoform Del-701	Y704	K.YC*RPESQEHPEADPGSAAPY@LK.T	0 1 1 1 0 1 0 1 0 0	0 0 0 0 0 0 0 0	0 0 0 0 0 0 0 0	0 0 0 0 0 0 0 0
Adhesion and Cytoskeleton	Q61140	p130cas	Y238	R.VGQGYVYEAAQTEQDEY@DTPR.H	0 2 1 3 0 1 2 0 1 0	2 2 1 0 1 1 0 1	0 0 0 0 0 0 0 0 0 0	0 0 0 0 0 0 0 0 1 0
	Q61140	p130cas	Y253	R.HLLAPGPQDIY@DVPPVR.G	4 5 6 4 1 4 1 3 0 3	1 0 0 0 0 0 0 0	2 2 3 1 1 0 1 0	0 0 0 0 0 0 0 0
	Q8VI36	Paxillin	Y88	R.YAHQQPPS^PLPVY@SSSAK.N	1 1 1 3 0 1 0 0 1 1	0 0 0 0 0 0 0 0	0 0 0 0 0 0 0 0	0 0 0 0 0 0 0 0
	Q8VI36	Paxillin	Y118	R.AGEEEHVY@SFPNK.Q	4 5 5 11 3 6 5 4 4 3	0 0 0 0 0 0 0 0	3 4 2 2 1 1 1 1 2	0 0 0 0 0 0 0 0
	Q9DBT6	Tensin	Y216	R.HAAYGGY@STPEDR.R	0 1 1 0 0 0 0 2 1 1	0 0 0 0 0 0 0 0	0 0 0 0 0 0 0 0 0 0	0 0 0 0 0 0 0 0 0 0
	Q8CJ95	Tensin 2	Y460	R.GPLDGSPY@AQVQR.V	1 1 1 3 1 1 0 1 0 0	2 0 0 0 0 0 0 0	0 0 0 0 0 0 0 0 0 0	0 0 0 0 0 0 0 0 0 0
	Q64727	Vinculin	Y821	K.SFLDSGY@R.I	2 2 2 3 0 1 2 1 1 1	0 0 0 0 0 0 0 0	0 0 0 0 0 0 0 0 0 0	0 0 0 0 0 0 0 0 0 0
	P30999	p120catenin	Y228	R.HYEDGYPGGSDNY@GSLSR.V	0 1 2 2 0 2 1 2 1 1	0 0 0 0 0 0 0 0	0 0 1 0 0 0 1 1 1	0 0 0 0 0 0 0 0
	Q80XQ4	p120catenin isoform	Y904	K.SLDNNY@STLNER.G	1 1 1 1 0 1 0 1 0 0	0 0 0 0 0 0 0 0	0 0 0 0 0 0 0 0 0 0	0 0 0 0 0 0 0 0 0 0
	Q99NH2	PARD3	Y719	R.ISHSLY@SGIEGLDESPTR.N	1 1 2 2 0 0 0 0 0 0	0 0 0 0 0 0 0 0	0 0 0 0 0 0 0 0 0 0	0 0 0 0 0 0 0 0 0 0
	Q68FH0	Plakophilin-4	Y477	R.NNYALNTAATY@AEPYRPVQYR.V	0 1 2 1 1 0 1 1 1 1	1 0 0 0 1 0 0 0	0 0 0 0 0 0 0 0 0 0	0 0 0 0 0 0 0 0 0 0
	Q91YD9	N-WASP	Y253	K.VIY@DFIEK.T	2 2 2 1 0 1 1 0 0 0	0 0 0 0 0 0 0 0	0 1 0 0 0 0 0 0 0 0	0 0 0 0 0 0 0 0 0 0
	Q75UV8	Sickle tail-b (Sickle tail-a)	Y244	R.NVY@YELNDVR.N	1 1 1 1 0 0 0 1 0 0	0 0 0 0 0 0 0 0	0 0 0 0 0 0 0 0 0 0	0 0 0 0 0 0 0 0 0 0
	Q75UV8	Sickle tail-b (Sickle tail-a)	Y393	R.NEGFY@ADPYLYHEGR.M	0 0 1 0 0 1 0 2 1 0	0 0 0 0 0 0 0 0	0 0 0 0 0 0 0 0 0 0	0 0 0 0 0 0 0 0 0 0
Others	Q62351	Transferrin receptor protein 1 - TfR	Y20	F.SNLFGGEPLSY@TRF.S	0 0 0 1 0 1 1 0 0 0	0 1 0 0 1 1 0 1	0 0 0 0 0 0 0 0 0 0	0 0 0 0 0 0 0 0 0 0
	Q8CFE6	Solute carrier family 38, member 2	Y41	K.SHY@ADVDPENQNFLLESNLGK.K	0 2 1 2 0 0 0 0 0 0	1 1 0 0 0 0 0 0	0 0 0 0 0 0 0 0 0 0	0 0 0 0 0 0 0 0 0 0
	P14869	60S acidic ribosomal protein P0	Y24	K.IIQLLDDY@PK.C	0 1 1 1 0 0 1 0 0 1	0 0 0 0 0 0 0 0	0 0 0 0 0 0 0 0 0 0	0 0 0 0 0 0 0 0 0 0
	Q8R143	Pituitary tumor-transforming gene 1 protein-interacting protein precursor	Y171	F.KEQNPY@EKF.-	0 1 1 0 0 0 0 0 0 0	1 0 1 1 0 0 0 0	0 0 0 0 0 0 0 0 0 0	0 0 0 0 0 0 0 0 0 0

[a] Peptides are shown in single letter amino acid code, with periods indicating cleavage sites; Y@, phosphotyrosine; S@, phosphoserine; S^ phosphoserine detected through neutral loss of phosphoric acid; C*, carboxyimidomethylated cysteine; M#, oxidated methionine. The position assigned to the pTyr site is based on the sequence of the given UniProt entry (ID #) for the protein. Numbers with shade-coded background indicate independent site identifications per round of analysis.

Table 3

Sites Detected with Significantly Higher Frequency in the Src-Transformed Cell Population[a]

	ID #	Protein Name	Site	Representative peptide	Nontransformed cells: trypsin 1 2 3 4 5 6 7 8 9 10	Nontransformed cells: chymotrypsin 11 12 13 14 15 16 17 18	Src-transformed cells: trypsin 1 2 3 4 5 6 7 8 9 10	Src-transformed cells: chymotrypsin 11 12 13 14 15 16 17 18
Signaling	Q80XU2	Src	Y92	R.AGPLAGGVTTFVALY@DYESR.T	0 0 0 0 0 0 0 0 0 0	0 0 0 0 0 0 0 0	3 0 1 6 6 0 0 1 1 0	13 1 1 1 0 1 1 1
	Q80XU2	Src	Y438	K.WTAPEAALY@GR.F	0 0 0 0 0 0 0 0 0 0	0 0 0 0 0 0 0 0	3 3 3 1 1 1 1 1 0 2	1 2 1 0 1 0 1 0 0
	P07356	Annexin-A2	Y274	L.YFADRLY@DSM.K	0 0 0 0 0 0 0 0 0 0	0 0 0 0 0 0 0 0	0 0 0 0 0 0 0 0 0 0	4 1 0 0 1 2 2 4
	P14824	Annexin-A6	Y29	R.GSVHDFPEFDANQDAEALY@TAMK.G	0 0 0 0 0 0 0 0 0 0	0 0 0 0 0 0 0 0	1 1 0 0 0 1 3 1 3 2	2 1 0 0 2 2 2 0
	P97465	Docking protein 1 - Dok1	Y401	R.LKEEGYELPY@NPATDDY@AVPPPR.S	0 0 0 0 0 0 0 0 0 0	0 0 0 0 0 0 0 0	1 2 1 2 2 2 1 0 1 1	0 0 0 0 0 0 0 0
	Q61598	Rab-GDP dissociation inhibitor beta	Y38	K.VLHMDQNPY@YGGESASITPLEDLYKR.F	0 0 0 0 0 0 0 0 0 0	0 0 0 0 0 0 0 0	4 4 3 3 3 3 3 2 3 2	1 0 0 0 0 0 0 0
Adhesion and Cytoskeleton	Q64727	Vinculin	Y99	K.LVQAAQMLQSDPY@SVPARDYLIDGSR.G	0 0 0 0 0 0 0 0 0 0	0 0 0 0 0 0 0 0	1 3 1 0 1 1 1 0 0 1	2 1 0 0 0 0 0 0
	P61161	Actin-like protein 2 - Arp2	Y91	K.HLWDY@TFGPEK.L	0 0 0 0 0 0 0 0 0 0	0 0 0 0 0 0 0 0	1 2 1 0 1 1 2 1 2 2	0 0 0 0 0 0 0 0
	Q9JM76	Arp2/3 complex subunit 3 - p21ARC	Y46	K.DTDIVDEAIY@YFK.A	0 0 0 0 0 0 0 0 0 0	0 0 0 0 0 0 0 0	1 0 0 0 1 0 1 1 1 1	1 0 1 0 1 1 2 1
	Q7TPR4	Alpha actinin 1	Y246	K.AIMTYVSSFY@HAFSGAQK.A	0 0 0 0 0 0 0 0 0 0	0 0 0 0 0 0 0 0	1 2 1 1 2 2 4 1 2 2	0 0 0 0 0 0 0 0
	Q80X90	Filamin-B	Y511	K.GFLDGVY@SFEYYPSTPGK.Y	0 0 0 0 0 0 0 0 0 0	0 0 0 0 0 0 0 0	2 2 2 0 2 2 1 2 2 2	0 0 0 0 0 0 0 0
	Q88342	Actin-interacting protein 1 - AIP1	Y237	K.AHDGGIY@AISWSPDSTHLLSASGDK.T	0 0 0 0 0 0 0 0 1 0	0 0 0 0 0 0 0 0	2 2 1 2 2 1 2 1 2 2	1 0 0 0 0 0 0 0
	Q6S394	Plectin-1	Y3250	R.ARQEEVY@SELQAR.E	0 0 0 0 0 0 0 0 0 0	0 0 0 0 0 0 0 0	2 2 3 2 2 0 2 2 1 1	0 0 0 0 0 0 0 0
Metabolic and biosynthetic enzymes	P17182	Enolase, alpha/beta/gamma	Y24	R.GNPTVEVDLY@TAK.G	0 0 0 0 0 0 0 0 1 0	0 0 0 0 0 0 0 0	9 18 13 15 10 0 2 3 1 2	15 4 3 2 0 1 1 1
	P17182	Enolase, alpha/beta/gamma	Y43	R.AAVPSGASTGIY@EALELR.D	1 1 1 2 0 0 0 0 1 0	0 0 0 0 0 0 0 0	6 12 8 8 7 3 1 2 3 2	11 4 2 5 1 3 1 2
	Q9DBJ1	Phosphoglycerate mutase 1	Y25	R.FSGWY@DADLSPAGHEEAK.R	0 0 0 1 0 0 0 0 1 0	0 0 0 0 0 0 0 0	2 2 3 4 2 2 1 1 2 2	0 1 0 1 0 0 0 0
	Q9CWJ9	Bifunctional purine biosynthesis protein	Y290	R.VC*MVY@DLYPTLTPLAVAYAR.A	0 0 0 0 0 0 0 0 1 0	0 0 0 0 0 0 0 0	1 2 4 3 3 4 4 3 5 1	1 0 0 0 0 0 0 0
	Q00612	Glucose-6-phosphate-1 dehydrogenase X	Y400	L.VIRVQPNEAVY@TKM.M	0 0 0 0 0 0 0 0 0 0	0 0 0 0 0 0 0 0	0 0 1 1 0 0 0 0 0 0	4 4 1 0 2 0 0 1
	Q00612	Glucose-6-phosphate-1 dehydrogenase X	Y506	R.VGFQYEGTY@K.W	0 0 0 0 0 0 0 0 0 0	0 0 0 0 0 0 0 0	0 1 0 0 0 4 2 1 3 2	0 0 0 0 0 0 0 0
	Q9JMH6	Thioredoxin-reductase-1, cytoplasmic	Y131	K.KVVYENAY@GR.F	0 0 0 0 0 0 0 0 0 0	0 0 0 0 0 0 0 0	2 3 3 4 3 0 0 0 0 0	0 0 0 0 0 0 0 0
RNA Synthesis/Processing	Q8C5L3	CCR4-NOT transcription complex subunit 2	Y43	K.FVEGVDSDYHDENMY@YSQSSMFPHR.S	0 0 0 0 0 0 0 0 0 0	0 0 0 0 0 0 0 0	1 1 3 0 2 2 2 0 2 2	0 0 0 0 0 0 2 1
	Q62167	ATP-dependent-RNA-helicase - DDX3X (DDX3Y, PL10)	Y68	K.DKDAY@SSFGSR.D	0 0 0 0 0 0 0 0 0 0	0 0 0 0 0 0 0 0	1 1 1 1 1 1 0 1 1 1	1 1 1 0 1 0 1 0
	Q62167	ATP-dependent-RNA-helicase - DDX3X (DDX3Y, PL10)	Y461	K.KGADSLEDFLY@HEGYAC*TSIHGDR.S	0 0 0 0 0 0 0 0 0 0	0 0 0 0 0 0 0 0	1 2 3 3 3 1 2 2 2 3	3 4 2 1 1 3 2 2
	Q91VC3	Probable ATP-dependent helicase - DDX48	Y202	K.GFKEQIY@DVYR.Y	0 0 0 0 0 0 0 0 0 0	0 0 0 0 0 0 0 0	2 2 2 2 2 0 2 0 1 1	0 0 0 0 0 0 0 0
	P70333	hnRNP H'	Y246	R.GAYGGGYGGYDDY@GGYNDGYGFGSDRFGR.D	0 0 0 0 0 0 0 0 0 0	0 0 0 0 0 0 0 0	1 1 1 0 1 1 1 2 2 2	1 0 0 0 0 1 0 0
	Q7TMK9	hnRNP Q	Y485	Y.RGGYEDPY@YGYEDF.Q	0 0 0 0 0 0 0 0 0 0	0 0 0 0 0 0 0 0	0 0 0 0 0 0 0 0 1 0	0 7 3 4 14 17 4 22 13
	Q91W59	RNA-binding motif, single-stranded-interacting protein 1	Y13	K.QQMYPQY@ATYYYPQYLQAK.Q	0 0 0 0 0 0 0 0 0 0	0 0 0 0 0 0 0 0	2 0 0 2 0 1 2 2 1 1	1 1 1 0 0 1 0 0 0
	Q91W59	RNA-binding motif, single-stranded-interacting protein 1	Y16	K.QQMYPQYATY@YYPQYLQAK.Q	0 0 0 0 0 0 0 0 0 0	0 0 0 0 0 0 0 0	2 2 3 3 2 2 0 1 1 1	0 0 0 0 0 0 0 0
	Q9Z108	Double-stranded RNA-binding protein Staufen homolog	Y404	R.TRPSEQLY@YLSR.A	0 0 0 0 0 0 0 0 0 0	0 0 0 0 0 0 0 0	1 3 2 3 1 2 2 1 1 2	0 0 0 0 0 0 0 0
Protein Synthesis/Processing	Q8CGC7	Bifunctional aminoacyl-tRNA synthetase	Y690	R.GFFIC*DQPYEPVSPY@SC*R.E	0 0 0 0 0 0 0 0 0 0	0 0 0 0 0 0 0 0	4 2 2 1 2 2 3 5 3 4	0 0 0 0 0 0 0 0
	Q640P8	Eukaryotic translation initiation factor 2A	Y362	K.LISKPVASDSTY@FAWC*PDGEHILTATC*APR.L	0 0 0 0 0 0 0 0 0 0	0 0 0 0 0 0 0 0	0 1 3 2 2 0 0 0 0 1	1 2 0 0 0 0 0 1
	Q8R1B4	Eukaryotic translation initiation factor 3, subunit 8	Y879	F.DHKQGTY@GGYF.R	0 0 0 0 0 0 0 0 0 0	0 0 0 0 0 0 0 0	0 0 1 0 0 0 0 0 0 0	3 1 2 1 2 1 1 2
	P60843	Eukaryotic translation initiation factor 4A-I	Y197	R.GFKDQIY@DIFQK.L	0 0 0 0 0 0 0 0 1 0	0 0 0 0 0 0 0 0	2 3 2 3 2 2 1 2 2 2	0 0 0 0 0 0 0 0
	Q91YE4	Eukaryotic translation initiation factor 3 subunit 6-interacting protein	Y72	K.TVSDLIDQKVY@ELQASR.V	0 0 0 0 0 0 0 0 0 0	0 0 0 0 0 0 0 0	2 2 2 3 2 2 4 3 2 2	1 1 0 1 0 0 0 0
	Q8BZQ7	Anaphase promoting complex subunit 2	Y825	R.DQQLIY@SAGVYRLPK.N	0 0 0 0 0 0 0 0 0 0	0 0 0 0 0 0 0 0	3 5 3 2 2 2 3 4 2 4	0 0 0 0 0 0 0 0
	Q9WUB0	Ubiquitin-conjugating enzyme 7-interacting protein 3	Y318	R.NSQEAEVAC*PFIDSTY@SC*PGK.L	0 0 0 0 0 0 0 0 0 0	0 0 0 0 0 0 0 0	1 1 1 2 0 2 2 1 1 1	0 0 0 0 0 0 0 0
	P49722	Proteasome subunit alpha type 2	Y75	K.HIGLVY@SGMGPDYR.V	0 0 0 0 0 0 0 0 1 0	0 0 0 0 0 0 0 0	6 5 4 6 5 4 4 3 2 3	6 5 3 1 4 3 4 4
	P49722	Proteasome subunit alpha type 2	Y100	R.KLAQQYYLVY@QEPIPTAQLVQR.V	0 0 0 0 0 0 0 0 0 0	0 0 0 0 0 0 0 0	5 3 4 6 4 4 6 6 3 2	4 0 1 0 1 0 0 0
	P70398	Probable ubiquitin carboxyl terminal hydrolase -FAF-X	Y2439	R.RPYTGNPQYTY@NNWSPPVQSNETSNGYFLER.S	0 0 0 0 0 0 0 0 0 0	0 0 0 0 0 0 0 0	1 3 1 1 1 1 3 1 4 4	0 0 0 0 0 0 0 0
Other	Q91VH2	Sorting-nexin-9	Y239	L.AKPKEKIAIIVGDY@GPM.W	0 0 0 0 0 0 0 0 0 0	0 0 0 0 0 0 0 0	0 0 0 0 1 0 0 0 0 0	3 1 1 1 1 2 3 3
	P62806	Histone H4	Y51	R.ISGLIY@EETR.G	0 0 0 0 0 0 0 0 0 0	0 0 0 0 0 0 0 0	2 2 1 1 1 0 1 1 1 1	1 0 0 0 0 0 0 0
	Q9EQU5	SET protein	Y145	R.IDFYFDENPY@FENK.V	0 0 0 0 0 0 0 0 0 0	0 0 0 0 0 0 0 0	1 3 3 2 3 0 1 1 1 1	2 1 0 1 0 0 0 0
	Q99J72	DNA dC->dU editing enzyme	Y255	K.HLC*Y@YHR.M	0 0 0 0 0 0 0 0 0 0	0 0 0 0 0 0 0 0	2 4 2 3 2 1 0 1 3 2	1 0 0 0 0 0 1 0
	P03355	MMLV Pol polyprotein	Y1118	L.AAAY@QEQLDRPVVPHPY@RVGDTVW.V	0 0 0 0 0 0 0 0 0 0	0 0 0 0 0 0 0 0	0 0 0 0 0 0 0 0 0 0	4 4 0 3 2 3 2 2
	P03355	MMLV Pol polyprotein	Y1142	R.WKGPY@TVLLTTPTALK.V	0 0 0 0 0 0 0 0 0 0	0 0 0 0 0 0 0 0	1 1 1 1 1 1 1 1 2 1	0 1 0 1 0 0 1 0
	UPI0000218B34	OUT domain-containing 4 protein	Y458	R.LLY@EIQNR.D	0 0 0 0 0 0 0 0 0 0	0 0 0 0 0 0 0 0	1 2 2 1 2 1 2 1 2 2	0 0 0 0 0 0 0 0
	Q5SSH7	Novel zinc finger protein	Y2706	K.WKDFELPGDTLY@YR.F	0 0 0 0 0 0 0 0 0 0	0 0 0 0 0 0 0 0	1 2 2 1 1 2 0 0 3 2	0 0 0 0 1 1 1 1
	Q91VX2	Ubiquitin-associated protein 2	Y853	R.LPMDY@YGIPFAAPTALASR.D	0 0 0 0 0 0 0 0 0 0	0 0 0 0 0 0 0 0	2 1 0 1 1 2 2 1 1 1	0 0 0 0 0 0 0 0
	Q91VX2	Ubiquitin-associated protein 2	Y876	R.DGNLANNPY@SGDVTK.F	0 0 0 0 0 0 0 0 0 0	0 0 0 0 0 0 0 0	1 1 2 1 0 0 1 1 1 1	2 3 1 0 1 1 0 1
	Q80X50	Ubiquitin-associated protein 2-like	Y612	Y.TSQNNAQGPLY@EQRSTQ.T	0 0 0 0 0 0 0 0 0 0	0 0 0 0 0 0 0 0	0 0 0 0 0 0 0 0 0 0	2 2 1 2 2 1 2 1
	Q80X50	Ubiquitin-associated protein 2-like	Y878	R.DGSLASNPY@SGDLTK.F	0 0 0 0 0 0 0 0 0 0	0 0 0 0 0 0 0 0	1 1 1 1 1 0 1 1 1 1	1 1 1 1 1 0 1 1 1 1

[a] See footnote for Table 2.

Table 4

Sites Detected Frequently in Both Nontransformed and Src-Transformed Cell Populations[a]

	ID #	Protein Name	Site	Representative peptide	Nontransformed cells: trypsin 1	2	3	4	5	6	7	8	9	10	Nontransformed cells: chymotrypsin 11	12	13	14	15	16	17	18	Src-transformed cells: trypsin 1	2	3	4	5	6	7	8	9	10	Src-transformed cells: chymotrypsin 11	12	13	14	15	16	17	18
Ssignaling	Q80XU2	Src (Fyn, Yes)	Y418	R.LIEDNEY@TAR.Q	1	1	1	2	1	1	0	1	1	2	0	0	0	0	0	0	0	0	3	1	3	2	2	2	3	2	1	1	1	1	0	1	1	1	1	1
	P34152-3	FAK	Y576	R.YM#EDSTY@YK.A	4	7	6	4	3	7	5	10	6	1	4	1	2	0	4	4	0	5	0	2	2	0	1	2	2	2	3	3	0	0	0	0	0	0	0	0
	P34152-3	FAK	Y577	R.YM#EDSTY@Y@K.A	0	2	2	1	1	3	1	6	4	1	1	0	1	0	2	1	0	1	0	0	0	0	0	0	0	0	2	2	0	0	0	0	0	0	0	0
	Q8BX56	Predicted protein kinase SqK269	Y632	K.VPIVINPNAY@DNLAIYK.S	4	2	4	3	0	0	0	0	0	0	0	0	0	0	0	0	0	0	1	2	2	1	2	0	1	1	0	0	1	0	0	1	0	0	1	0
	Q8BX56	Predicted protein kinase SqK269	Y638	K.NAIKVPIVINPNAY@DNLAIY@K.S	1	1	2	1	0	0	0	0	0	0	0	0	0	0	0	0	0	0	1	3	2	1	2	0	1	1	0	0	1	0	0	1	0	0	1	0
	P35235	Tyrosine phosphatase SHP-2	Y62	K.IQNTGDY@YDLYGGEK.F	0	0	1	1	0	1	1	1	0	1	1	0	0	0	0	1	0	0	2	1	1	2	1	0	1	0	0	0	1	1	1	1	1	1	1	1
	P26450	PI3K p85alpha	Y467	K.SREYDRLY@EEYTR.T	0	0	1	1	0	0	0	1	1	0	0	0	0	0	0	0	0	0	0	1	1	0	0	1	0	1	1	1	0	0	0	0	0	0	0	0
	Q9JLL7	Inositol phosphatase SHIP2	Y987	K.NSFNNPAY@YVLEGVPHQLLPLEPPSLAR.A	2	1	2	2	0	0	1	0	0	0	0	0	0	0	0	0	0	0	0	0	1	1	1	0	1	3	1	1	0	0	0	0	0	0	0	0
	Q68FF6	GIT1	Y554	R.LQPFHSTELEDDAIY@SVHVPAGLYR.I	1	1	1	1	1	0	4	0	1	1	1	1	1	0	1	1	0	1	3	6	2	3	3	2	3	5	3	2	1	1	1	1	1	1	1	1
	Q91YM2	p190RhoGAP	Y943	R.NEEENIY@SVPHDSTQGK.I	2	3	2	7	2	2	3	3	2	2	0	0	0	0	0	0	0	0	2	3	2	3	1	2	2	1	2	2	0	0	0	0	0	0	0	0
	Q921Q7	RIN1	Y35	K.EKPSTDPLY@DTPDTR.G	0	0	0	2	0	0	1	0	1	0	0	0	0	0	0	0	0	0	1	1	1	0	0	0	0	0	0	0	1	0	0	0	0	0	0	0
	P07356	Annexin A2	Y23	K.LSLEGDHSTPPSAY@GSVKPYTNFDAER.D	1	0	1	2	0	0	0	0	0	0	2	3	3	0	0	1	0	0	1	1	0	1	1	0	0	1	1	0	2	3	1	3	0	1	0	1
	P59672	ANKS1/Odin	Y471	L.AVRPRIQSSAPQEEEEHPY@EL.L	0	0	0	0	0	0	0	0	0	0	0	3	1	1	0	1	1	0	0	2	1	0	0	0	0	0	0	0	1	0	0	2	0	0	1	
	P49817	Caveolin-1	Y14	K.YVDSEGHLY@TVPIR.E	1	1	1	1	0	1	0	1	1	0	0	0	0	0	0	0	0	0	1	1	1	1	1	1	0	0	0	0	0	0	0	0	0	0	0	0
	P97465	Dok1	Y314	R.IPPGPSQDSVY@SDPLGSTPAGAGEGVHSK.K	0	1	0	2	0	0	1	0	0	0	0	0	0	0	0	0	0	0	1	1	0	1	1	1	1	1	1	1	0	0	0	0	0	0	0	0
	P97465	Dok1	Y361	K.LTDSKEDPIY@DEPEGLAPAPPR.G	3	5	5	5	2	4	4	5	5	4	3	1	2	1	2	1	1	1	5	5	5	4	4	2	1	2	1	2	1	1	0	0	0	0	0	1
	P97465	Dok1	Y408	R.LKEEGYELPYNPATDDY@AVPPPR.S	1	1	2	2	0	2	1	1	1	1	0	0	0	0	0	0	0	0	0	2	1	2	2	1	2	0	1	1	0	0	0	0	0	0	0	0
	Q99M51	NCK1	Y105	K.RKPSVPDTASPADDSFVDPGERLY@DLNMPAFVK.F	0	0	0	0	0	0	0	1	0	2	1	0	0	0	0	0	0	0	0	1	1	1	2	2	0	0	0	0	2	0	0	0	0	0	0	0
	P98083	SHC1	Y423	R.ELFDDPSY@VNIQNLDK.A	4	1	4	2	1	2	1	1	3	1	0	0	0	0	0	0	0	0	1	1	1	1	0	1	1	0	1	1	0	0	0	0	0	0	0	0
Adhesion and Cytoskeleton	Q61140	p130cas	Y253	R.HLLAPGPQDIY@DVPPVR.G	4	5	6	4	1	4	1	3	0	3	1	0	0	0	0	0	0	0	2	2	3	1	1	0	1	0	0	0	0	0	0	0	0	0	0	0
	Q61140	p130cas	Y271	R.GLLPNQYGQEVY@DTPPMAVK.G	1	2	1	1	0	0	0	0	1	0	0	0	0	0	0	0	0	0	0	2	0	2	0	0	1	1	0	0	0	0	0	0	0	0	0	0
	Q61140	p130cas	Y414	R.VLPPEVADGSVVDDGVY@AVPPPAER.E	1	0	1	2	0	0	1	0	1	0	0	0	0	0	0	0	0	0	2	3	2	1	0	1	2	1	4	3	0	0	0	0	0	0	0	0
	Q8BFW7	Lipoma preferred partner -LPP	Y245	Y.MAGPSSGQIY@GPGPRGY.N	0	0	0	0	0	0	0	0	0	0	5	4	3	0	1	0	0	1	0	0	0	0	0	0	0	0	0	0	5	3	1	1	0	0	0	0
	Q8BFW7	Lipoma preferred partner -LPP	Y301	R.YYEPY@YAAGPSYGGR.S	0	1	1	1	0	1	1	1	1	1	0	0	0	0	0	0	0	0	1	3	2	1	1	1	3	1	1	1	1	0	0	0	0	0	0	0
	Q8BFW7	Lipoma preferred partner -LPP	Y302	R.YYEPYY@AAGPSYGGR.S	1	1	1	1	0	1	0	1	1	1	0	0	0	0	0	0	0	0	2	1	2	2	1	1	3	1	1	1	0	0	0	0	0	0	0	0
	Q8VI36	Paxillin	Y118	R.AGEEEHVY@SFPNK.Q	4	5	5	11	3	6	5	4	4	3	0	0	0	0	0	0	0	0	3	4	2	2	1	1	1	1	1	2	0	0	0	0	0	0	0	0
	P26039	Talin-1	Y26	K.TMQFEPSTMVY@DAC*R.M	1	1	2	0	0	1	0	0	0	0	1	1	0	0	1	0	0	0	1	1	2	2	2	0	0	0	1	1	0	1	0	0	0	0	0	0
	P26039	Talin-1	Y70	K.ALDY@YMLR.N	0	1	2	0	0	0	0	1	0	1	1	2	0	0	2	1	0	1	0	1	2	1	1	3	1	0	0	0	0	0	0	0	0	0	0	0
	P30999	p120 catenin	Y96	K.LNGPQDHNHLLY@STIPR.M	0	0	2	3	1	2	0	2	1	1	0	0	0	0	0	0	0	0	3	3	2	2	1	0	1	1	1	1	0	0	0	0	0	0	0	0
	P30999	p120 catenin	Y228	R.HYEDGYPGGSDNY@GSLSR.V	0	1	2	2	0	2	1	2	1	1	0	0	0	0	0	0	0	0	0	0	1	0	0	0	0	1	1	1	0	0	0	0	0	0	0	0
	P39447	Tight junction protein ZO-1	Y1164	R.HEEQPAPAY@EVHNR.Y	1	1	1	0	0	1	0	1	0	1	0	0	0	0	0	0	0	0	1	1	1	1	1	1	1	0	1	1	1	0	0	0	0	0	0	0
	P18760	Cofilin-1	Y139	K.HELQANC*Y@EEVKDR.C	1	1	1	2	1	1	1	1	0	0	1	0	1	0	0	0	0	0	1	2	1	1	1	0	1	1	1	1	0	0	0	0	0	0	0	0
	Q60598	Cortactin	Y466	Y.TSEPVY@ETTEAPGHY.Q	0	0	0	0	0	0	0	0	0	0	2	1	1	1	1	1	1	1	0	0	0	0	0	0	0	0	0	0	3	3	1	1	2	2	2	2
	P42208	Septin-2	Y17	K.QQPTQFINPETPGY@VGFANLPNQVHR.K	0	1	2	1	0	1	0	0	0	0	0	0	0	0	0	0	0	0	0	1	0	1	1	1	1	2	0	1	0	0	0	0	0	0	0	0
	P70460	VASP	Y39	R.VQIY@HNPTANSFR.V	0	2	1	1	0	0	0	0	0	0	1	0	0	0	0	0	0	0	0	1	2	1	0	0	1	0	0	0	1	1	0	0	0	0	0	0
Other	P17182	Alpha-enolase	Y43	R.AAVPSGASTGIY@EALELR.D	1	1	1	2	0	0	0	0	1	0	0	0	0	0	0	0	0	0	6	12	8	8	7	3	1	2	3	2	11	4	2	5	1	3	1	2
	P16858	GAPDH	Y315	K.LISWYDNEY@GYSNR.V	1	1	1	2	0	1	0	0	2	0	0	0	0	0	0	0	0	0	3	4	2	2	3	5	4	4	3	4	2	0	0	0	0	1	2	2
	P10126	Elongation factor 1-alpha 1 eEF1A-1 (eEF1A-2)	Y29	K.STTTGHLIY@K.C	1	1	1	1	1	1	2	1	1	1	0	0	0	0	0	0	0	0	2	2	2	2	2	1	3	2	1	1	0	0	0	0	0	0	0	0
	P10126	Elongation factor 1-alpha 1 eEF1A-1 (eEF1A-2)	Y141	R.EHALLAY@TLGVK.Q	0	0	1	1	0	0	0	1	1	0	0	0	0	0	0	0	0	0	1	0	1	1	0	0	1	0	0	0	0	0	0	0	0	0	0	0
	P22682	E3 ubiquitin protein ligase - Cbl	Y672	K.PSSSANAIY@SLAARPLPMPK.L	0	1	0	0	1	0	1	0	1	0	0	0	0	0	0	0	0	0	2	0	1	0	0	0	1	0	0	0	0	0	0	0	0	0	0	0
	Q9Z0R6	Intersectin-2	Y921	R.GEPEALY@AAVTK.K	1	2	2	2	1	2	1	2	1	1	0	0	0	0	0	0	0	0	3	2	1	3	0	0	0	0	0	0	0	0	0	0	0	0	0	0
	Q920I4	Carnitine deficiency-associated protein CDV3A (CDV3B)	Y213	R.KTPQGPPEIY@SDTQFPSLQSTAK.H	0	0	1	2	1	0	1	1	0	0	0	0	0	0	0	0	0	0	1	3	1	1	1	1	1	1	1	1	1	1	0	0	0	0	0	0
	UPI00005125B7	PREDICTED: similar to Oligophrenin 1	Y371	K.LWLEAMDGKEPIY@TLPAIISK.K	0	2	1	2	1	0	0	0	0	0	0	0	0	0	0	0	0	0	2	1	0	0	0	1	0	1	0	1	0	0	0	0	0	0	0	0

[a] Sites found ≥4 times in both cell populations (CMGC kinases excluded). Numbers with color-coded background indicate site identifications for each round of analysis. Proteins and pTyr sites implicated from past studies as well-documented or likely Src substrates are highlighted in red.

Table 5

SILAC Quantification of Sites Frequently Detected in Both Cell Populations[a]

protein (site)[b]	peptide[c]	ratio (H/L)[d]
CDK1 (Y15)[N]	IEKIGEGTY@GVVYK	0.51
	IGEGTY@GVVYK	0.55
GSK3 β (Y216)[N]	GEPNVSY@IC*SR	1.1
p190RhoGAP (Y943)[N]	NEEENIY@SVPHDSTQGK	2.8
p130Cas (Y253)[N]	HLLAPGPQDIY@DVPPVR	4.0
RIN1 (Y35)	EKPSTDPLY@DTPDTR	5.0
Talin (Y26)	TMQFEPSTMVY@DAC*R	6.2
Talin (Y70)	ALDY@YMLR	6.5
eEF1A-1 (Y29)	STTTGHLIY@K	9.0
VASP (Y39)	VQIY@HNPTANSFR	9.0
p120ctn (Y96)	LNGPQDHNHLLY@STIPR	10.5
Enolase α (Y43)[S]	AAVPSGASTGIY@EALELR	H only
	AAVPSGASTGIY@EALELRDNDKTR	8.9
GAPDH (Y315)	LISWYDNEY@GYSNR	12.5
Src (Y418)	LIEDNEY@TAR	32

[a] Shown are sites that were also identified ≥4 times in both nontransformed and Src-transformed cells in the label-free analysis. The complete list of SILAC sites is given in Supplemental Table S3.

[b] N, site highly enriched in nontransformed cells by spectral count analysis; S, site highly enriched in Src-transformed cells by spectral count analysis.

[c] Y@, pTyr; C*, carboxyimidomethylated cysteine

[d] Ratio (heavy/light) of peptide MS peak from Src-transformed cells relative to the same peptide from nontransformed cells. H only, peptide peak evident only in Src-transformed cells.